Accepted Manuscript

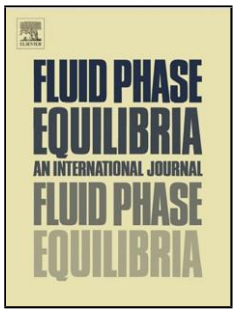

Title: Modeling of asphaltene precipitation from *n*-alkane diluted heavy oils and bitumens using the PC-SAFT equation of state

Author: Mar´ıa A. Zu´niga-Hinojosa Daimler N. Justo-Garc˜ ´ıa Marco A. Aquino-Olivos Luis A. Roman-Ram´´ırez Fernando Garc´ıa-Sanchez´

PII: S0378-3812(14)00337-9
DOI: http://dx.doi.org/doi:10.1016/j.fluid.2014.06.004
Reference: FLUID 10147

To appear in: *Fluid Phase Equilibria*

Received date: 7-4-2014
Revised date: 30-5-2014
Accepted date: 2-6-2014

Please cite this article as: M.A. Zu´niga-Hinojosa, D.N. Justo-Garc˜ ´ia, M.A. AquinoOlivos, L.A. Roman-Ram´ ´irez, F. Garc´ia-Sanchez, Modeling of asphaltene precipitation´ from *n*-alkane diluted heavy oils and bitumens using the PC-SAFT equation of state, *Fluid Phase Equilibria* (2014), http://dx.doi.org/10.1016/j.fluid.2014.06.004

Modeling of asphaltene precipitation from *n*-alkane diluted heavy oils and bitumens using the PC-SAFT equation of state

María A. Zúñiga-Hinojosa[1], Daimler N. Justo-García[2], Marco A. Aquino-Olivos[3], Luis A. Román-Ramírez[4], and Fernando García-Sánchez[1,1]

[1] Laboratorio de Termodinámica, Programa de Investigación en Ingeniería Molecular, Instituto Mexicano del Petróleo. Eje Central Lázaro Cárdenas 152, 07730 México, D.F., México.

[1] Corresponding author. Tel.: +52 55 9175 6574. E-mail: fgarcias@imp.mx

[2] Departamento de Ingeniería Química Petrolera, ESIQIE, Instituto Politécnico Nacional, Unidad Profesional Adolfo López Mateos, 07738 México, D.F., México.

[3] Programa de Aseguramiento de la Producción de Hidrocarburos, Instituto Mexicano del Petróleo. Eje Central Lázaro Cárdenas 152, 07730 México, D.F., México.

[4] School of Chemical Engineering, University of Birmingham, Edgbaston, Birmingham B15 2TT, United Kingdom.

ABSTRACT

In this work, the PC-SAFT equation of state was applied to the modeling of asphaltene precipitation from *n*-alkane diluted heavy oils and bitumens. Liquid-liquid equilibrium was assumed between a dense liquid phase (asphaltene-rich phase) and a light liquid phase. The liquid-liquid equilibrium calculation, in which only asphaltenes were allowed to partition to the dense phase, was performed using an efficient method with Michelsen's stability test. The bisection or Newton-Raphson method was used to improve convergence. Experimental information of the heavy oils and bitumens, characterized in terms of solubility fractions (saturates, aromatics, resins, and asphaltenes), was taken from the literature. Asphaltenes were divided into fractions of different molar masses using a gamma distribution function. Predictions of the PC-SAFT equation of state using linear correlations of the binary interaction parameters between asphaltene subfractions and the *n*-alkane were compared with the measured onset of precipitation and the amount of precipitated asphaltene (fractional yield) of the heavy oils and bitumens diluted with *n*-alkanes. Results of the comparison showed a satisfactory agreement between the experimental data and the calculated values with the PC-SAFT equation.

Key words: onset; asphaltene precipitation; equation of state; PC-SAFT; liquid-liquid equilibrium.

---

1. Introduction

Asphaltenes are defined as the fraction of crude oil or bitumen that precipitates with the addition of a low-chain liquid *n*-alkane (*n*-pentane or *n*-heptane) and dissolves in aromatic solvents as toluene or benzene. In practice, there are different aspects of the asphaltene precipitation that are important for the oil industry such as the prevention of the plugging in transport pipelines and the damages caused in the refinery facilities due to the asphaltene precipitation process. A major problem is when different crude oils having different densities and viscosities are mixed and they are, in turn, mixed with light liquid hydrocarbons (e.g., natural gasolines) to reduce the viscosity of the crude oil blends, since asphaltene precipitation may occur due to the instability of the crude oil mixtures [1].

To overcome such a problem, various research groups have developed different approaches to predict and quantify the onset and amount of precipitated asphaltene in crude oils. This task was started with the approach of Hirschberg et al. [2], who applied the regular solution theory for modeling asphaltene precipitation in crude oils. Later, this modeling approach was improved by other authors to predict (1) the amount of precipitated asphaltene from *n*-alkane diluted heavy oils and bitumens [3, 4], (2) the asphaltenes dissolved in pure solvents [5, 6], and (3) the stability of crude oil blends [1, 7]. In particular, Yarranton and co-workers [1, 3, 4] proposed approaches to predict asphaltene precipitation by treating them as a mixture of subfractions with different densities and molar masses. These approaches have been successfully applied to several heavy oils and bitumens diluted with *n*-alkanes [3, 4]. The heavy oils and bitumens were characterized based on SARA analysis and the polidispersity of the asphaltene fraction was included through the use of a gamma distribution function.

Other approaches in which the asphaltene precipitation is understood as a result of self-assembly and instability of resinous-asphaltene aggregates in the crude oil have also been used. For instance, Leontaritis and Mansoori [8] presented a colloidal model based on the assumption that the insoluble solid asphaltene particles are suspended in the crude oil; the suspended solid asphaltene particles being stabilized by the adsorbing resins on their surface. In this model, resins are necessary for the asphaltenes to exist in solution. Subsequently, Victorov and Firoozabadi [9], Pan and Firoozabadi [10], and Victorov and Smirnova [11], among others, presented thermodynamic models to predict asphaltene precipitation in petroleum fluids by assuming that asphaltene precipitation from petroleum fluid is a micellization process. These models, however, although have shown promising results in explaining most of the experimentally observed results, they are still far from provides satisfactory quantitative representation.

On the other hand, the application of an equation of state to calculate the asphaltene solubility in solvents was studied by Gupta [12] considering a solid-liquid equilibrium calculation. Nghiem and co-workers [13-15] applied a modeling technique based on the representation of the precipitated asphaltene as a pure dense phase. In this approach, the heaviest component in the oil is divided into two fractions, the nonprecipitating and the precipitating fraction. The precipitating fraction is considered as pure asphaltenes and the prediction precipitation process is quantified by a three phase flash calculation. Sabbagh et al. [16] applied in their approach a liquid-liquid equilibrium calculation, where one of the liquid phases is considered a light phase or a non-precipitating phase and the other liquid phase is considered a heavy liquid phase or a precipitating phase. The precipitating phase is considered a phase where only asphaltenes are present. They used the PR

equation of state [17] to represent the asphaltene-rich liquid phase by relating the equation of state parameters of each asphaltene fraction to monomer parameters using group contribution theory. Ting et al. [18] modeled the asphaltene phase behavior in a model live oil and a recombined oil under reservoir conditions by using the SAFT equation of state [19]. In this case, the parameters of the equation of state for the asphaltenes were adjusted to precipitation data from oil titrations with *n*-alkanes at ambient conditions.

By using a molecular-thermodynamic framework based on the SAFT equation of state and colloidal theory, Wu et al. [20, 21] calculated the solubility of asphaltenes in petroleum liquids as a function of temperature, pressure, and liquid-composition. In this approach, asphaltenes and resins were represented by pseudo-pure components while all other components in the solution were represented by a continuous medium that affects interactions among asphaltene and resin particles. The effect of the medium on asphaltene-asphaltene, resin-asphaltene, and resin-resin pair interactions was taken into account through its density and dispersion-force properties. The SAFT model was used in the framework of McMillanMayer theory, which considers hard-sphere repulsive, association and dispersion-force interactions. In their calculations, Wu et al. assumed that asphaltene precipitation is a liquid-liquid equilibrium process.

Buenrostro-Gonzalez et al. [22] used an approach similar to that suggested by Wu et al. for modeling the asphaltene precipitation from *n*-alkane diluted Mexican crude oils. They used the statistical association fluid theory for potentials of variable range (SAFT-VR) equation of state [23] in the framework of the McMillan-Mayer theory in the calculations to represent the asphaltene precipitation envelopes and bubble point pressures of the two oils investigated. By matching a single titration curve or two precipitation onset

points with this SAFT-VR equation of state, satisfactory predictions of asphaltene precipitation over wide temperature, pressure, and composition intervals were obtained.

Li and Firoozabadi applied the cubic-plus-association (CPA) equation of state [24] to study the asphaltene precipitation from solutions of toluene and an *n*-alkane and from *n*-alkane diluted heavy oils and bitumens [25], and the asphaltene precipitation in live oils from temperature, pressure, and composition effects [26]. Heavy oils and bitumens were characterized in terms of saturates, aromatics/resins, and asphaltenes, whereas the live oils were characterized by considering the pure components, the pseudohydrocarbon components, and the hydrocarbon residue. In the case of heavy oils and bitumens, the asphaltene precipitation was modeled as liquid-liquid equilibrium. By using a single adjustable parameter −the cross

association energy between asphaltene and aromatics/resins (or toluene), the amount of asphaltene was successfully predicted over a broad range of temperatures, pressures, and compositions for *n*-alkane diluted model solutions, heavy oils, and bitumens. In the case of live oils, the asphaltene precipitation was modeled as liquid-liquid equilibrium between the upper onset and bubble point pressures and as gas-liquid-liquid equilibrium between the bubble point and lower onset pressures. The amount and onset pressures of asphaltene precipitation in several live oils were reasonably reproduced over a broad range of composition, temperature, and pressure conditions.

More recently, Panuganti et al. [27] presented a procedure to characterize crude oils and plot asphaltene envelopes using the PC-SAFT equation of state. The results obtained with the proposed characterization method showed a satisfactory matching with the experimental data points for the bubble point and asphaltene precipitation onset curves studied.

The aim of this work is to apply the PC-SAFT equation of state [28] to predict the asphaltene precipitation from *n*-alkane diluted heavy oils and bitumens by using linear correlations of the binary interaction parameter as a function of *n*-alkane concentration. It is assumed that there exists liquid-liquid equilibrium coexistence between a light non-precipitating liquid phase and a heavy precipitating liquid phase, where only asphaltenes are allowed to partition, and that the effect of self-association is included in the asphaltene molar mass distribution to model the asphaltene precipitation from solvent diluted heavy oils and bitumens. The oils are characterized in terms of saturates, aromatics, resins, and asphaltenes (SARA) fractions, and the asphaltenes are, in turn, treated as nano-aggregates formed from asphaltene monomers and divided into subfractions of different aggregation number based on a gamma distribution function.

2. Thermodynamic model

2.1 PC-SAFT equation of state

In the PC-SAFT equation of state [28], the molecules are considered to be chains composed of spherical segments, in which the pair potential for the segment of a chain is given by a modified square-well potential [29]. Non-associating molecules are characterized by three pure component parameters, namely, the temperature-independent segment diameter σ, the depth of the potential ε, and the number of segments per chain m.

The PC-SAFT equation of state written in terms of the Helmholtz energy for an N-component mixture of non-associating chains consists of a hard-chain reference contribution and a perturbation contribution to account for the attractive interactions. In terms of reduced quantities, this equation can be expressed as

$$\tilde{a}^{res} = \tilde{a}^{hc} + \tilde{a}^{disp} \tag{1}$$

The hard-chain reference contribution is given by

$$\tilde{a}^{hc} = \langle m \rangle \tilde{a}^{hs} - \sum_{i=1}^{N} x_i (m_i - 1) \ln g_{ii}^{hs}(d_{ii}) \tag{2}$$

where $\langle m \rangle$ is the mean segment number in the mixture,

$$\langle m \rangle = \sum_{i=1}^{N} x_i m_i \tag{3}$$

The Helmholtz energy of the hard-sphere fluid is given on a per-segment basis as

$$\tilde{a}^{hs} = \frac{1}{\zeta_0}\left[\frac{3\zeta_1\zeta_2}{(1-\zeta_3)} + \frac{\zeta_2^3}{\zeta_3(1-\zeta_3)^2} + \left(\frac{\zeta_2^3}{\zeta_3^2} - \zeta_0\right)\ln(1-\zeta_3)\right] \tag{4}$$

and the radial distribution function of the hard-sphere fluid is

$$g_{ijhs}(d_{ij}) = \frac{1}{(1-\zeta_3)} + \left(\frac{d_i d_j}{d_i + d_j}\right)\frac{3\zeta_2}{(1-\zeta_3)^2} + \left(\frac{d_i d_j}{d_i + d_j}\right)^2 \frac{2\zeta_2^2}{(1-\zeta_3)^3} \tag{5}$$

with ζ_n defined as

1 ⎛ d d ⎞ 3 ⎛ d d ⎞ 2 2

$$\zeta_n = \frac{\pi}{6}\rho\left(\sum_{i=1} x_i m_i d_i^n\right) \qquad n = 0,1,2,3 \tag{6}$$

The temperature-dependent segment diameter d_i of component i is given by

$$d_i = \sigma_i\left[1 - 0.12\exp\left(-3\frac{\varepsilon_i}{kT}\right)\right] \tag{7}$$

where k is the Boltzmann constant and T is the absolute temperature.

The dispersion contribution to the Helmholtz energy is given by

$$\tilde{a}^{disp} = -2\pi\rho \cdot I_1(\eta,\langle m\rangle)\cdot\langle m^2\varepsilon\sigma^3\rangle - \pi\rho\cdot\langle m\rangle C_1 \cdot I_2(\eta,\langle m\rangle)\cdot\langle m^2\varepsilon^2\sigma^3\rangle \tag{8}$$

where C is an abbreviation for the compressibility factor, defined as

$$C_1 = \left[1 + Z^{hc} + \rho\frac{\partial Z^{hc}}{\partial\rho}\right]^{-1} = \left(1 + \langle m\rangle\frac{8\eta - 2\eta^2}{(1-\eta)^4} + (1-\langle m\rangle)\frac{20\eta - 27\eta^2 + 12\eta^3 - 2\eta^4}{[(1-\eta)(2-\eta)]^2}\right)^{-1} \tag{9}$$

where Z^{hc} is the compressibility factor of the hard-chain reference contribution and η is the reduced density, and

$$\langle m^2\varepsilon\sigma^3\rangle = \sum_{i=1}^{N}\sum_{j=1}^{N} x_i x_j m_i m_j\left(\frac{\varepsilon_{ij}}{kT}\right)\sigma_{ij}^3 \tag{10}$$

$$\langle m^2\varepsilon^2\sigma^3\rangle = \sum_{i=1}^{N}\sum_{j=1}^{N} x_i x_j m_i m_j\left(\frac{\varepsilon_{ij}}{kT}\right)^2\sigma_{ij}^3 \tag{11}$$

where the term in angular brackets, $\langle\cdots\rangle$, represents a mixture property.

The parameters for a pair of unlike segments are obtained by using conventional combining rules

$$\sigma_{ij} = \frac{1}{2}(\sigma_i + \sigma_j) \tag{12}$$

$$\varepsilon_{ij} = \varepsilon_i\sqrt{\varepsilon_j}(1 - k_{ij}) \tag{13}$$

where k_{ij} is a binary interaction parameter, which is introduced to correct the segment-segment interactions of unlike chains.

The terms $I_1(\eta,\langle m\rangle)$ and $I_2(\eta,\langle m\rangle)$ in Eq. (8) are calculated by simple power series in density

$$I_1(\eta,\langle m\rangle) = \sum_{i}^{6} a_i\cdot\eta^i \tag{14}$$

$i=0$ $i=0$

$$I_2(\eta,\langle m\rangle) = \sum_{i=0}^{6} b_i \cdot \eta^i \tag{15}$$

where the coefficients a_i and b_i depend on the chain length as given in Gross and Sadowski [28].

The density to a given system pressure p^{sys} is determined iteratively by adjusting the reduced density η until $p^{cal} = p^{sys}$. For a converged value of η, the number density of molecules ρ, given in Å^{-3}, is

$$\rho = \frac{\eta}{\pi}\left(\sum_i x_i m_i d_i^3\right)^{-1} \tag{16}$$

Using Avogadro's number and appropriate conversion factors, ρ produces the molar density in $^{-3}$.

The pressure can be calculated in units of Pa $=$ N $\cdot$ m^{-2} by applying the relation

$$p = Z\,kT\rho\left(10^{10}\,\frac{\text{Å}}{m}\right)^3 \tag{17}$$

from which the compressibility factor Z, can be derived.

The expression for the fugacity coefficient is given by

$$\ln\phi_i = \tilde{a}^{res} + \left(\frac{\partial a^{res}}{\partial x_i}\right)_{T,v,x_{j\neq i}} - \sum_{k=1}^{N}\left[x_k\left(\frac{\partial a^{res}}{\partial x_k}\right)_{T,v,x_{j\neq k}}\right] + (Z-1) - \ln Z \tag{18}$$

calculated from

6 (N

different units such as kmol·m

(
\

~ ~

where the derivatives with respect to mole fractions are calculated regardless of the summation relation $\sum_{i=1}^{N} x_i =$ 1.

3. Solution procedure

For purposes of modeling, the heavy oils and bitumens were divided into pseudo-components based on SARA (saturates, aromatics, resins, and asphaltenes) fractions. Asphaltenes were, in turn, divided into pseudo-components based on a molar mass distribution function, whereas saturates, aromatics, and resins fractions are considered to be a single pseudo-component. Thus, the self-association of the asphaltenes is considered in the model used here to calculate the amount of asphaltene precipitation from *n*-alkane diluted heavy oils and bitumens.

3.1 Asphaltene molar mass distribution

By considering the asphaltenes to be macromolecular aggregates of monodispersed asphaltene monomers, there is a distribution of aggregate sizes (molar mass) in which asphaltenes can be divided into fractions of different molar mass. In this case, the asphaltene fraction was divided into 30 subfractions, each representing a different aggregate size range described by an aggregation number

$$r = \frac{M}{M_m} \tag{19}$$

where r is the aggregation number of each asphaltene molar mass fraction, M is the molar mass of the asphaltene aggregate, and M_m is the monomer molar mass of the asphaltenes.

The gamma distribution function, as reported by Yarranton and co-workers [1, 16, 30], was chosen to describe the molar mass distribution of the aggregates. The gamma distribution function is given by

$$f(r) = \frac{1}{M_m \Gamma(\alpha)} \left[(r-1)\right]^{\alpha} (r-1)^{\alpha-1} \exp\left[-\left[\alpha((r-1)/r)\right]\right] \quad (20)$$

where r is the average aggregation number given by M/M_m; M being the average molar of the selfassociated asphaltene, and α is a parameter that determines the shape of the distribution.

Sabbagh et al. [16] used a value of $\alpha = 4$ for the precipitation of asphaltenes from diluted heavy oils and bitumens with relatively low average molar mass asphaltenes. They used an asphaltene average monomer molar mass of 1800 g/mol and adjusted the average molar mass for the diluted heavy oils and bitumens. Asphaltene self-association was accounted for by using the average associated molar mass of the asphaltene estimated for the given precipitation conditions. The maximum molar mass was set to 30,000 g/mol.

For the modeling purposes of *n*-alkane diluted heavy oils and bitumens with the PC-SAFT model, the α parameter used in this work was set to 9.5. The other parameters used were those reported by Sabbagh et al. [16], with the exception of the maximum molar mass, which was set to 15,000 g/mol.

The distribution was discretized into increments of constant Δr. The mass fraction of each segment was calculated from the expression [3]

$$w_i = \frac{\int_{r_i}^{r_{i+1}} f(r)dr}{\int_{r_n}^{r_1} f(r)dr} \tag{21}$$

whereas the average aggregation parameter for each fraction was calculated as

$$\bar{r}_i = \frac{\int_{r_i}^{r_{i+1}} rf(r)dr}{\int_{r_i}^{r_{i+1}} f(r)dr} \tag{22}$$

from which the average molar mass of each asphaltene fraction can be calculated as

$$M_i = \bar{r}_i M_m \tag{23}$$

3.2 Liquid-liquid equilibrium calculation

As stated earlier, the asphaltene precipitation modeling is based on a liquid-liquid flash calculation, where the denser liquid phase is assumed to be the asphalt phase (precipitant phase) and the lighter one the non-precipitant phase formed of maltenes (i.e., saturates, aromatics, and resins fractions) and of an n-alkane. The procedure reported by Sabbagh [31] was adopted here for calculating asphaltene precipitation.

The equilibrium calculation assumes equality of fugacities of two liquid phases at a given temperature and pressure. The process is iterative in which at each step the fugacity of all components in each phase is calculated and compared. The equilibrium constants are then updated until convergence is achieved when the liquid phase fugacities are equal. Fig. 1 presents a schematic flow diagram of the algorithm for the equilibrium calculation.

The iterative process implies solving for the number of moles of the precipitant liquid phase β, the wellknown Rachford-Rice equation [32]

$$f(\beta) = \sum_{i=1}^{N} \frac{z_i((K_i - 1))}{1 + \beta(K_i - 1)} = 0 \quad (24)$$

where K_i is the liquid-liquid equilibrium ratio and z_i, x_i, and y_i are the mole fractions of component i in, respectively, the feed, the first (light) liquid phase, and the second (dense) liquid phase. Fig. 2 shows the algorithm for the Rachford-Rice flash calculation. It can be seen in this figure that a bisection method (e.g., the Brent method [33]) can be used instead of Newton-Raphson method to improve convergence. This is due to the very large K-values of the asphaltene fractions which, sometimes, makes difficult to apply the Newton-Raphson method.

Equation (24) yields a physically correct root for $0 < \beta < 1$ using constant K-values determined in an outer loop. Once the value of β is determined, mole fractions of each component in every phase are calculated from the relations

$$X_i = \frac{z^i}{1 + \beta(K_i - 1)} \quad (25)$$

$$Y_i = \frac{z^i K^i}{1 + \beta(K_i - 1)} = X_i K_i \quad (26)$$

where X_i and Y_i are non-normalized mole fractions and their summations $\sum_{i=1}^{N} X_i$ and $\sum_{i=1}^{N} Y_i$ are equal to one when convergence is achieved.

In this algorithm, the K-values are updated in an outer loop after each iteration, since they depend on the composition of each phase, which is not known before convergence.

The updating procedure in based on the equilibrium conditions

$$f_{iL1} = f_{iL2} \qquad i = 1, \ldots, N \quad (27)$$

where f_i^{L1} and f_i^{L2} are, respectively, the fugacities of component i at the first and second liquid phases, and the convergence criteria that satisfies the stability test [34]

$$\ln f_i - \ln f_{iz} = \theta \qquad i = 1, \ldots, N \quad (28)$$

where f_i is the fugacity of component i for a new potential phase and f_{iz} is the reference fugacity of component i in all the existing phases. Equation (28) can be written as

$$i \qquad iz \qquad \left| \overline{\varphi_z z_i} \right|$$

$$\theta_x = -\ln \sum_{j=1}^{N} X_j$$

which is valid for any phase.

On the other hand, the method reported by Sabbagh [31] to establish the stability criteria at equilibrium is

$$= f_{iy} \qquad i = 1,\ldots, N$$

$$\varphi \; x \; p = \varphi_{iy} y_i p \qquad i = 1,\ldots, N$$

and the equilibrium ratios, which can be expressed as

$$\frac{y_i}{x_i} = \frac{\varphi_x}{\varphi_y} = \frac{y_i f_{ix}}{x_i f_{iy}} \qquad i = 1,\ldots, N$$

$$\left(\frac{f_{ix}}{f_{iy}} \right) + \ln\left(\frac{y_i}{x_i} \right) \qquad i = 1,\ldots, N$$

where X_i and Y_i are obtained from the solution of the Rachford-Rice, and x_i and y_i are their normalized mole fractions. Consequently, Eq. (34) can also be written as

$$\left(\frac{Y_i}{X_i} \right) - \left(\ln f_{iy} + \ln \sum_{j=1}^{N} Y_j - \ln f_{ix} - \ln \sum_{j=1}^{N} X_j \right) \qquad i = 1,\ldots, N$$

or

$$\theta_x = \ln f - \ln f = \ln \left| \begin{pmatrix} \varphi_{ix} x_i \end{pmatrix} \right| \qquad (29)$$

or

(30)

given by

f_{ix} (31) or

$_{ix}$ $_{i}$ (32)

$K_i =$ (33)

or

$\ln K_i = \ln$ (34)

$\ln K_i = \ln$ (35)

$\ln K_i = \ln|| \overline{X^{Y_i}}_i ||J - \left[\ln f_{iy} - \theta_y - \ln f_{ix} + \theta_x\right] \qquad i = 1,..., N$ (36)

If the equilibrium ratios K_i at iteration k are defined as

$K_i^{(k)} = \left(Y_i / X_i\right)^{(k)} \qquad i = 1,..., N$ (37)

then the equilibrium ratios K_i at iteration $(k+1)$ can be calculated as follows

$\ln K_{i(k+1)} = \ln K_{i(k)} - g_i \qquad i = 1,..., N$ (38)

where

$$g_i = \ln f_{iy} - \theta_y - \ln f_{ix} + \theta_x \qquad i = 1,..., N \tag{39}$$

Equation (38) is based on the successive substitution method, which has linear convergence rate. To accelerate the convergence, a suitable step length γ can be used. In such a case, Eq. (38) is written as

$$\ln K_i^{(k+1)} = \ln K_i^{(k)} - \gamma g_i \qquad i = 1,..., N \tag{40}$$

where γ is set equal to unity at the start of calculations and it is modified using an appropriate numerical method during the iteration process.

To use the procedure outlined above, the *K*-values must be initialized. This is done by first setting the *K*values of all components, except for the asphaltene fractions, to zero. Then, the *K*-values for the asphaltene subfractions are initialized by assuming the mole fractions of the light liquid phase equal to the mole fractions of feed components (except for the asphaltenes), and calculating the mole fractions of components of the dense liquid phase from the molar masses and mass fractions of the asphaltene fractions. The *K*-values are then calculated from the ratio of the asphaltene pseudo-components mole fractions in the dense liquid phase to the mole fractions of the same pseudo-components in the light liquid phase.

During the liquid-liquid flash calculation, the Rachford-Rice equation is solved for the moles of the dense liquid phase by using the Newton-Raphson method or a bisection method to obtain convergence. After convergence, the component mole fractions of each phase are calculated using the updated *K*-values and the obtained moles of the dense liquid phase are used to calculate the mass of the dense liquid phase (the precipitate) in order to determine the fractional yield of asphaltene precipitation, defined as the mass of precipitated asphaltenes and solids divided by the mass of the heavy oil or bitumen [16]. In this procedure, fugacities of the components in the two liquid phases were calculated with the PC-SAFT equation of state.

2.3 Determination of asphaltenes PC-SAFT parameters

The correlations reported in the literature for estimating the three pure-component parameters (i.e., number of segments per chain m , temperature-independent segment diameter σ, and depth of the potential ε)

characterizing the PC-SAFT equation of state for asphaltenes, are valid for asphaltene subfractions of molar masses up to 1475 g/mol [35]. However, these correlations cannot be used to estimate such parameters for asphaltenes that can reach very high molar masses, e.g., 15,000 g/mol.

The use of the gamma distribution function to split the asphaltenes SARA fraction into subfractions indicates that the first asphaltene subfraction −the one with the smallest molar mass of the subfractions– should be greater than the monomer molar mass value. The molar masses of the different subfractions were obtained from the difference between the largest molar mass (set to 15,000 g/mol) and the monomer molar mass, divided by the number of subfractions; i.e., 30. For the heavy oils and bitumens studied here, the monomer molar mass value was set to 1800 g/mol [16], All these molar mass values are beyond the range of validity of the reported correlations to estimate the PC-SAFT parameters m , σ, and ε for asphaltene subfractions.

This aspect is illustrated in Fig. 3, which shows the PC-SAFT parameters m , σ, and ε/k for saturates pseudo-component as a function of the molar mass calculated from the correlations reported by Panuganti et al. [27,36]. As can be seen in this figure, parameters σ and ε/k tend to reach an asymptotic value as the molar mass increases. If these correlations were used to calculate parameters σ and ε/k for the asphaltene subfractions at molar masses greater than, say 2000 g/mol, all the subfractions would have similar σ and ε/k values, which is not desired in practice. It is therefore necessary that parameters σ and ε/k increase as the molar mass of the asphaltene subfraction increases.

To circumvent this problem, we suggest the following empirical correlations for estimating the PC-SAFT parameters m , σ, and ε/k as a function of the molar mass of each asphaltene subfraction:

$$m = 0.0257M + 0.8444 \quad (41)$$

$$\sigma = 0.1097\ln M + 3.3685 \quad (42)$$

$$\varepsilon/k = 32.81\ln M + 80.398 \quad (43)$$

where M is the molar mass of the asphaltene subfraction, and parameters σ, and ε/k are given in units of Å and Kelvin, respectively, whereas parameter m is dimensionless.

The correlations given by Eqs. (41)−(43) allow estimating the PC-SAFT parameters m , σ, and ε/k to represent the several asphaltene subfractions resulting from the gamma distribution function. It should be

mentioned that these correlations were developed by assuming that the asphaltene subfractions behave as long linear chains of carbons molecules. Of course, this does not correspond to the real structural form of any asphaltenes fraction; however, it is just a "practical" way to conceive and approximate the structural form of the asphaltenes to predict with the PC-SAFT model the complex phase behavior of the asphaltene precipitation process experimentally exhibited from *n*-alkane diluted heavy oils and bitumens.

Table 1 presents the PC-SAFT parameters m , σ, and ε/k calculated from correlations (41)−(43) for the "hypothetical" asphaltene subfractions used in this work. These parameters are also plotted in Fig. 3. This figure shows that, according to correlations (41)−(43), parameter m increases linearly as the molar mass increases, while parameters σ and ε/k increase in a regular trend as the molar mass increases without reaching an asymptotic value.

On the other hand, because the saturates, aromatics, and resins fractions obtained from the SARA analysis are considered to be pseudo-components with molar masses not greater than 1100 g/mol for the heavy oils and bitumens studied, it seems reasonable to use the correlations suggested by Panuganti et al. [27, 36] to estimate the PC-SAFT parameters m , σ, and ε/k for these pseudo-components. That is, the following correlations were used

$$m = 0.0257M + 0.8444 \tag{44}$$

$$\sigma = 4.047 - (4.8013 \ln M)/M \tag{45}$$

$$\varepsilon/k = \exp(5.5769 - 9.523/M) \tag{46}$$

for saturates pseudo-component, and

$$m = (1-\gamma)(0.0223M + 0.751) + \gamma(0.0101M + 1.7296) \tag{47}$$

$$\sigma = (1-\gamma)(4.1377 - 38.1483/M) + \gamma(4.6169 - 93.98/M) \tag{48}$$

$$\varepsilon/k = (1-\gamma)(0.00436M + 283.93) + \gamma(508 - 234100/M) \tag{49}$$

for aromatics + resins pseudo-component, where γ is the degree of aromaticity that determine the tendency of the aromatics + resins pseudo-component to behave as a poly-nuclear aromatic ($\gamma = 1$) or as a benzene derivative component ($\gamma = 0$) [37]. Here, it is assumed that the heavy oils and bitumens have a low degree of aromaticity, so that we set the aromaticity factor γ to 0.01 to estimate the PC-SAFT parameters m , σ, and ε/k for aromatics and resins pseudo-components.

Fig. 4 shows the calculated m , σ, and ε/k parameters for saturates, aromatics, and resins pseudocomponents as a function of the molar mass. The PC-SAFT parameters for aromatics and resins pseudocomponents were calculated (1) by assuming that the resins pseudo-component behaves as a poly-nuclear aromatic and the aromatics pseudo-component as a benzene derivative component (solid lines), and (2) by using an aromaticity factor of 0.01 (dashed lines). This figure also shows the PC-SAFT parameters for asphaltenes calculated from correlations (41)−(43). Also showed in this figure are the calculated PCSAFT parameters for saturates, aromatics, and resins fractions with corresponding molar masses of 460, 522, and 1040 g/mol (solid square symbols) [16] by using an aromaticity factor of 0..01 for the aromatics and resins pseudo-components.

3.4 Estimation of interaction parameters

It is typical in equation of state calculations to introduce binary interactions (BIPs) for modeling the phase behavior of complex systems such as exhibited by the system heavy oil (or bitumen)-solvent. In this case, the BIPs are used between the heaviest most polar component (asphaltenes) and the lightest, least polar component (the *n*-alkane). The interaction parameters between different asphaltene subfractions are set to zero, and they are considered to have similar structures. The BIPs between asphaltenes and *n*-alkane are assumed to be the same for all the asphaltene subfractions. Thus, the only interaction parameter used in the modeling is the one corresponding to the interaction between asphaltene and n-alkane. All other interactions parameters between asphaltenes + saturates, asphaltenes + aromatics, asphaltenes + resins, saturates + aromatics, saturates + resins, and aromatics + resins pseudo-components, aromatics + nalkanes, and resins + n-alkanes, are set to zero.

The BIPs are generally determined by minimizing the difference between the model predictions and the experimental data. Therefore, to increase the usefulness of the combining rule given in Eq. (13), we have determined the binary interaction parameter k_{ij} characterizing the interactions between the asphaltene

subfractions and the *n*-alkane for the PC-SAFT equation of state by minimizing the difference between the experimental fractional yields (amount of precipitated asphaltene) and those ones calculated with the PC-SAFT model for different concentrations of *n*-alkane.

The simplex optimization procedure of Nelder and Mead [38] was used in the computations by searching the minimum of the following objective function

$$F_{obj} = \sum_{i=1}^{M} \left(\frac{Y_{iexp} - Y_{ical}}{Y_{iexp}} \right)^2 \quad (50)$$

where $(Y_i^{exp} - Y_i^{cal})$ is the difference between the experimental and calculated values of fractional yields for an experiment i, and M is the total number of experimental data.

In a first attempt, we used all the asphaltene fractional yield data reported by Sabbagh et al. [16] to obtain a single binary interaction for each bitumen or heavy oil, independent of temperature or composition. However, we found a rather poor agreement between the experimental fractional yields and those values calculated with the PC-SAFT model, so that we realized than a single interaction parameter was not enough to give a good representation of the experimental fractional yield data for any of the seven *n*alkane diluted bitumens and heavy oils investigated in this work. Therefore, to follow the behavior of these interaction parameters as a function of the *n*-alkane mass fraction, we adjusted the interaction parameter for each fractional yield datum (i.e., $M = 1$). This is illustrated in Figs. 5 and 6.

Fig. 5 shows the behavior of the interaction parameter as a function of the *n*-alkane mass fraction from the Athabasca bitumen diluted with *n*-pentane, *n*-hexane, and *n*-heptane at 296.2 K and 0.1 MPa. This figure shows that all the interaction parameters are negative but they become less negative as the concentration of the *n*-alkane increases. In this case, the interaction parameter values varied from (−0.008 to −0.002), (−0.0067 to −0.0057), and (−0.0057 to −0.0041), for *n*-pentane, *n*-hexane, and *n*-heptane, respectively.

Fig. 5 also shows that there exists a great deal of scatter among the adjusted interaction parameters, may be due to possible experimental errors in the method of determining the asphaltene fractional yields. Notwithstanding this fact, they were correlated to the following straight line

$$k_{ij} = a \cdot w_{n-alk} + b \quad (51)$$

where k_{ij} is the binary interaction parameter between asphaltenes and the *n*-alkane and it is assumed that they are the same for all the asphaltene subfractions, w_{n-alk} is the *n*-alkane mass fraction, and a and b are

the two constants of the correlation. Although the values of the interaction parameters are in general small, they are very sensitive when these are used to calculate the fractional yield at a given *n*-alkane composition, as will be discussed below.

Fig. 6 shows the behavior of the interaction parameter as a function of the *n*-alkane mass fraction from the Athabasca bitumen diluted with *n*-heptane at 273.2 and 0.1 MPa, and at 296.2, 323.2, and 373.2 K all at 2.1 MPa. This figure shows the effect of temperature and pressure upon the behavior of the interaction parameters as a function of the *n*-heptane. As seen in this figure, the interaction parameters are negative at the lower temperatures, irrespective of the pressure, varying from (−0.0095 to −0.0059) and (−0.0061 to −0.0042) as the *n*-alkane concentration increases, similar to those showed in Fig. 5. However, as temperature increases, the slope of the straight line changes from positive to negative. That is, the interaction parameters varying from (−0.0013 to −0.0030) and (0.0020 to −0.0024) at 323.2 and 373.2 K both at 2.1 MPa, respectively, as the *n*-alkane concentration increases. This indicates that the influence of temperature is stronger than pressure when correlating the fractional yield data for this bitumen diluted with *n*-heptane. The same behavior is observed for the Cold Lake bitumen diluted with *n*-heptane at 296.2 and 323. 2 K both at 2.1 MPa, and at 373.2 K and 6.9 MPa

Table 3 presents the estimated constants *a* and *b* of the linear correlations to calculate the interaction parameters for asphaltene−*n*-alkane interactions of Athabasca, Cold Lake, Lloydminster, Venezuela 1, Venezuela 2, Russia and Indonesia bitumens and heavy oils, where the *n*-alkane is either *n*-pentane, or *n*hexane, or *n*-heptane. They are listed according to Figs. 9−20 presented in Sabbagh et al.'s article [16].

4. Modeling results and discussion

To investigate the ability of the PC-SAFT equation of state to predict asphaltene precipitation, the procedure suggested by Sabbagh et al. [16] was used for calculating asphaltene fractional yields of Athabasca, Cold Lake, Lloydminster, Venezuela 1, Venezuela 2, Russia and Indonesia bitumens and heavy oils diluted with *n*-alkanes. In all the calculations, the PC-SAFT equation of state was used as the thermodynamic model to represent the liquid phases in conjunction with interaction parameters estimated from Eq. (51). The characteristic parameters m , σ, and ε/k for saturates, aromatics and resins pseudo

components, and for asphaltene subfractions, are given in Table 1, while those corresponding to the precipitating compounds (*n*-pentane, *n*-hexane, and *n*-heptane) were taken from Gross and Sadowski [28].

SARA analysis fractions (in weight %) and asphaltene average associated molar masses for the seven bitumens and heavy oils studied in this work are given in Table 2. The average molar mass reported by Sabbagh et al. for each SARA fraction are 460, 522, 1040, and 1800 g/mol for saturates, aromatics, resins, and asphaltenes (monomer), respectively. Results from the modeling of the bitumens and heavy oils diluted with an *n*-alkane (*n*-pentane, or *n*-hexane, or *n*-heptane) at several conditions of temperature and pressure, are given below.

4.1 n-Alkane diluted heavy oils and bitumens

Figs. 7 13 show the measured asphaltene fractional yields from Athabasca, Cold Lake, Lloydminster, Venezuela 1, Venezuela 2, Russia and Indonesia bitumens and heavy oils diluted with *n*-alkanes (*n*pentane, *n*-hexane, and *n*-heptane) at 296.2 K and atmospheric pressure, and those ones calculated with the PC-SAFT equation of state at the same conditions of temperature and pressure. As seen in these figures, the calculated fractional yields are in good agreement with the experimental ones when they are calculated using interaction parameters that depend on the *n*-alkane mass fraction as given by Eq. (51).

By using the PR equation of state [17] with interaction parameters between asphaltene subfractions and the *n*-alkane, independents of temperature and *n*-alkane concentration, Sabbagh et al. [16] obtained a reasonable representation of the asphaltene fractional yields for these heavy oils and bitumens diluted with *n*-pentane, *n*-hexane and *n*-heptane. However, the representation of the asphaltene fractional yields for the heavy oils and bitumens diluted with *n*-pentane was rather poor. Although, they claim that, in most cases, the average absolute deviation was less than 0.02 (fractional yield) and that the greatest discrepancies occurred at high *n*-pentane mass fractions, possibly due to that (1) the model did not account for the partition of the resins to the dense phase, (2) there was a significant mass of trapped maltenes (i.e., saturates, aromatics, and resins) at the high fractional yields measured in *n*-pentane, and (3) the formation of multiple liquid and/or solid phases that were not accounted for in the modeling, it is clear that a single interaction parameter independent of temperature and solvent concentration is not enough to adequately represent the experimental data of asphaltene precipitation irrespective of the equation of state used, as shown in Figs. 5 and 6. Of course, it is also possible that these discrepancies may be due to errors in the experimental data as pointed out by Sabbagh et al.

Similar results were obtained by Li and Firoozabadi [25] when they modeled the asphaltene precipitation for the same heavy oils and bitumens using the CPA equation of state [24]. They characterized the heavy oils and bitumens in terms of saturates, aromatics/resins, and asphaltenes. In this model, the physical interactions were described by the PR equation of state [17] and the self-association between asphaltenes and aromatics/resins were represented by the thermodynamic perturbation theory of Wertheim [39-42]. The model contains only one adjustable parameter, namely, the cross energy between asphaltenes and aromatics/resins molecules that depends on the types of asphaltenes and *n*-alkane, and probably temperature, but is independent of pressure and *n*-alkane concentration. Through the adjustment of this parameter, they reproduced most of the experimental fractional yield data. However, for *n*-pentane at high mass fractions, the fractional yield was always underestimated, in spite of considering in their model the partitioning of resins to the dense liquid phase rich in asphaltenes.

Figs. 7−13 also show that the PC-SAFT predictions of the fractional yields for both low and high *n*pentane concentrations are in very good agreement with the experimental data and that the discrepancies existing between the experimental and calculated fractional yields may be due to experimental errors and not to the ability of the equation of state in modeling this type of systems.

The PC-SAFT equation of state has also successfully been used to modeling the asphaltene precipitation process of several *n*-alkane diluted Mexican oils and their blends at 296.2 K and atmospheric pressure, which experimentally exhibit a large region of "colloidal stability" as a function of the *n*-alkane mass fraction. This wide region both limits and delays the asphaltene precipitation process. The results of the modeling will be presented in a subsequent communication.

4.2 n-Alkane diluted heavy oils and bitumens as a function of temperature

Figs. 14−16 show the effect of temperature on the experimental and calculated asphaltene fractional yields from Athabasca and Cold Lake bitumens diluted with *n*-heptane, and from Venezuela 1 heavy oil diluted with *n*-pentane, respectively. Fig. 14 presents the results of the modeling obtained with the PCSAFT equation of state at 273.2 K and 0.1 MPa, and at 296.2, 323.2 and 373.2 K all at 2.1 MPa, whereas Fig. 15 shows the results of the modeling realized at 296.2 and 323.2 K both at 2.1 MPa, and 373.2 K and

6.9 MPa. These figures show, in general, that there exists a good agreement between the experimental and Page

calculated asphaltene fractional yields, except at 373.2 K where the representation of the experimental data is rather poor, may be due to some experimental difficulties to obtain consistent data at this temperature, as pointed out by Sabbagh et al. [16]. These figures also show that the asphaltene fractional yield decreases as temperature increases, irrespective of the pressure.

Fig. 16 presents the results of the modeling at 273.2 and 296.2 K both at 0.1 MPa. An examination of this figure shows that there is a poor agreement between the experimental and calculated asphaltene fractional yields for the two sets of experimental data. These discrepancies are due to that the adjusted interaction parameters do not follow a linear trend in function of the *n*-pentane mass fraction, so that it was not possible to obtain a suitable linear correlation from these interaction parameters. For instance, the adjusted interaction parameter at 296.2 K, which correctly matches the experimental asphaltene fractional yield, was −0.00713 for an *n*-pentane mass fraction of 0.3832, but this interaction parameter becomes more negative as the *n*-pentane mass fraction increases up to reach a value of about 0.6. Then, the interaction parameters turn back to be less negative as the *n*-pentane mass fraction increases reaching a value of −0.00557 at an *n*-pentane mass fraction of 0.9267. Consequently, the interaction parameter estimated from the linear correlation given by Eq. (51) was not able to correctly predict the asphaltene fractional yield at the *n*-pentane mass fraction of 0.3832, as can be seen in this figure. This example illustrates the strong effect of the interaction parameters in predicting the asphaltene precipitation for the heavy oils and bitumens studied in this work.

4.3 n-Alkane diluted heavy oils and bitumens as a function of pressure

Figs. 17−18 show the effect of pressure on the experimental and calculated asphaltene fractional yields from the Athabasca and Cold Lake bitumens, respectively, diluted with *n*-heptane at 296.2 K and pressures of 0.1, 2.1, and 6.9 MPa. These figures show that the asphaltene fractional yields obtained with the PC-SAFT equation of state are, on the whole, in good agreement with the experimental data for both bitumens diluted with *n*-heptane. Also observed in these figures is the little effect of pressure on the experimental and calculated asphaltene fractional yields; the experimental and calculated fractional yields decrease only

slightly with pressure for both bitumens. This indicates that the effect of temperature on the asphaltene fractional yields is stronger than the effect of pressure.

Finally, it is worth mentioning that the modeling results of asphaltene precipitation show a decrease in the amount of precipitated asphaltene at high *n*-alkane fractions (high dilution) for most of the figures presented above (see Figs. 7-18), whereas the experimental data points follow a different trend. As can be seen in these figures, the PC-SAFT EoS is able to give good results both for the onset point at which the precipitation begins and for the fractional yields at different *n*-alkane mass fractions (usually less than 0.9). These figures also show that at high n-alkane mass fractions, the model predicts a maximum in the fractional yield, but at higher *n*-alkane mass fractions a decrease in the precipitated asphaltene is observed. An explanation of this behavior is that, in thermodynamic models, the asphaltenes have a small solubility in *n*-alkanes. However, at very high *n*-alkane mass fractions, the concentration of asphaltenes in the system is very small and the small amount that remains soluble reduces the amount of precipitated asphaltene, so that the decreasing in the fractional yield is a result of dilution effects that become dominant.

5. Conclusions

The ability of the PC-SAFT thermodynamic model to predict the asphaltene precipitation process obtained by the addition of an *n*-alkane to seven bitumens and heavy oils at different conditions of temperature and pressure was investigated. The results obtained showed that this equation of state is able to satisfactorily represent the precipitation process of the asphaltenes for these bitumens and heavy oils by using linear correlations for the binary interaction parameters of asphaltene (subfractions)−*n*-alkane as a function of the *n*-alkane mass fraction.

Liquid-liquid equilibrium was assumed between a dense liquid phase (asphaltene-rich phase), which only asphaltenes were allowed to partition, and a light liquid phase. The calculated fractional yields showed to be very sensitive to the interaction parameter value. The heavy oils and bitumens were characterized in terms of saturates, aromatics, resins, and asphaltenes fractions. The saturates, aromatics, and resins fractions were considered as single pseudocomponents, whereas the asphaltenes fraction was divided into subfractions of different molar mass based on a gamma distribution function. The use of a gamma

distribution function considering the self-aggregation of the asphaltenes through the average associated molar mass, proved to be suitable for representing the molar mass distribution of the asphaltene subfractions for the PC-SAFT equation of state.

Acknowledgments

The authors thank the financial support of the Sectorial Fund CONACyT-SENER (Hydrocarbons) under Project Y.00118. D. N. Justo-García gratefully acknowledges the National Polytechnic Institute for their financial support through the Project SIP-20130658**.** M. A. Zúñiga-Hinojosa thanks the National Council for Science and Technology of Mexico (CONACyT) and the Mexican Petroleum Institute for their pecuniary support through a Ph.D. fellowship.

References

[1] A. K. Tharanivasan, W. Y. Svrcek, H. W. Yarranton, S. D. Taylor, D. Merino-Garcia, P. M. Rahimi. Energy Fuels 23 (2009) 3971−3980.

[2] A. Hirschberg, L. N. J. deJong, B. A. Schipper, J. G. Meijer. Soc. Pet. Eng. J. 24 (1984) 283−293.

[3] H. Alboudwarej, K. Akbarzadeh, J. Beck, W. Y. Svrcek, H. W. Yarranton. AIChE J. 49 (2003) 2948−2956.

[4] K. Akbarzadeh, H. Alboudwarej, W. Y. Svrcek, H. W: Yarranton. Fluid Phase Equilib. 232 (2005) 159−170.

[5] S. I. Andersen. Pet. Sci. Technol. 12 (1984) 1551−1577.

[6] H. W. Yarranton, J. H. Masliyah. AIChE J. 42 (1996) 3533−3543.

[7] J. S. Buckley, J. Wang, J. L. Creek. In: Asphaltenes, Heavy Oils, and Petroleomics, O. C. Mullins, E. Y. Sheu, A. Hammami, Eds., Springer Publishing, New York, pp. 401−437, 2007.

[8] K. J. Leontaritis, G. A. Mansoori. Paper SPE 16258 presented at the 1987 SPE Intl. Symposium on Oilfield Chemistry, San Antonio, Texas, 4-6 February, 1987.

[9] A. I. Victorov, A. Firoozabadi. AIChE J. 42 (1996) 1753−1764.

[10] H. Pan, A. Firoozabadi. SPE Production & Facilities 13 (1998) 118−127.

[11] A. I. Victorov, N. A. Smirnova. Fluid Phase Equilib. 158-160 (1999) 471−480.

[12] A. K. Gupta. M. Sc. Thesis, University of Calgary, Calgary, Alberta, Canada, 1986.

[13] L. X. Nghiem, M. S. Hassam, R. Nutakki, A. E. D. George. Paper SPE 26642 presented at the 68th Annual Technical Conference and Exhibition of the Society of Petroleum Engineers, Houston, Texas, 3-6 October 1993.

[14] L. X. Nghiem, D. A. Coombe. SPE J. 2 (1997) 170−176.

[15] B. F. Khose, L. X. Nghiem, H. Maeda, K. Ohno. Paper SPE 64465 presented at the SPE Asia Pacific Oil and Gas Conference and Exhibition, Brisbane, Australia, 16–18 October 2000.

[16] O. Sabbagh, K. Akbarzadeh, A. Badamchi-Zadeh, W. Y. Svrcek, H. W. Yarranton. Energy Fuels 20 (2006) 625−634.

[17] D.-Y. Peng, D. B. Robinson. Ind. Eng. Chem. Fundam. 15 (1976) 59−64.

[18] P. D. Ting, G. J. Hirasaki, W. G. Chapman. Pet. Sci. Technol. 21 (2003) 647−661.

[19] W. G. Chapman, K. E. Gubbins, G. Jackson, M. Radosz. Ind. Eng. Chem. Res. 29 (1990) 1709− 1721.

[20] J. Wu, J. M. Prausnitz, A. Firoozabadi. AIChE J. 44 (1998) 1188−1199.

[21] J. Wu, J. M. Prausnitz, A. Firoozabadi. AIChE J. 46 (2000) 197−209.

[22] E. Buenrostro-Gonzalez, C. Lira-Galeana, A. Gil-Villegas, J. Wu. AIChE J. 50 (2004) 2552−2570.

[23] A. Gil-Villegas, A. Galindo, P. J. Whitehead, S. Mills, G. Jackson. J. Chem. Phys. 106 (1997) 4168−4186.

[24] G. M. Kontogeorgis, E. C. Voutsas, I. V. Yakoumis, D. P. Tassios. Ind Eng. Chem. Res. 35 (1996) 4310−4318.

[25] Z. Li, A. Firoozabadi. Energy Fuels 24 (2010) 1106−1113.

[26] Z. Li, A. Firoozabadi. Energy Fuels 24 (2010) 2956−2963.

[27] S. R. Panuganti, F. M. Vargas, D. L. Gonzalez, A. S. Kurup, W. G. Chapman. Fuel 93 (2012) 658−669.

[28] J. Gross, G. Sadowski. Ind. Eng. Chem. Res. 40 (2001) 1244−1260.

[29] S. S. Chen, A. Kreglewski. Ber. Bunsenges. Phys. Chem. 81(1977) 1048−1052.

[30] K. Akbarzadeh, A. Dhillon, W. Y. Svrcek, H. W. Yarranton. Energy Fuels 18 (2004) 1424−1441.

[31] O. Sabbagh. M.Sc. Thesis, University of Calgary, Calgary, Alberta, Canada, 2004.

[32] H. H. Rachford, J. D. Rice. Petrol. Trans. AIME 195 (1952) 327−328.

[33] W. H. Press, S. A. Teukolsky, W. T. Vetterling, B. P. Flannery. Numerical Recipes in Fortran: The Art of Scientific Computing, 2nd ed., Cambridge University Press, New York, 1992.

[34] R. A. Heidemann, M. L. Michelsen. Ind. Eng. Chem. Res. 34 (1995) 958−966.

[35] M. Tavakkoli, S. R. Panuganti, V. Taghikhani, M. R. Pishvaie, W. G. Chapman. Fuel 117 (2014) 206−217.

[36] S. R. Panuganti, M. Tavakkoli, F. M. Vargas, D. L. Gonzalez, W. G. Chapman. Fluid Phase Equilib. 359 (2013) 2−16.

[37] D. L. Gonzalez, G. J. Hirasaki, W. G. Chapman. Energy Fuels 21 (2007) 1231−1242.

[38] J. A. Nelder, R. A. Mead. Comput. J. 7 (1965) 308−313.

[39] M. S. Wertheim. J. Stat. Phys. 35 (1984) 19−34. [40] M. S. Wertheim. J. Stat. Phys. 35 (1984) 35−47.

[41] M. S. Wertheim. J. Stat. Phys. 42 (1986) 459−476. [42]

M. S. Wertheim. J. Stat. Phys. 42 (1986) 477−492.

Table 1. PC-SAFT parameters for saturates, aromatics, and resins pseudo-components, [a] and asphaltene subfractions. [b]

Component	*M* g/mol	*m*	σ Å	ε/*k* K
Saturates	460.0	12.6664	3.9830	258.84 Aromatics
522.0	12.3377	4.0683	288.23 Resins	1040.0
23.8259	4.1053	290.59		
Asph. subfract. 1	2191.6	57.1696	4.2124	332.79
Asph. subfract. 2	2569.4	66.8784	4.2298	338.00
Asph. subfract. 3	2956.6	76.8296	4.2452	342.61
Asph. subfract. 4	3364.8	87.3189	4.2594	346.85
Asph. subfract. 5	3785.5	98.1314	4.2723	350.72
Asph. subfract. 6	4213.0	109.1177	4.2840	354.23
Asph. subfract. 7	4644.3	120.2028	4.2947	357.43
Asph. subfract. 8	5078.0	131.3484	4.3045	360.35
Asph. subfract. 9	5513.2	142.5331	4.3136	363.05
Asph. subfract. 10	5949.4	153.7445	4.3219	365.55
Asph. subfract. 11	6385.4	164.9749	4.3297	367.88
Asph. subfract. 12	6823.9	176.2193	4.3370	370.05
Asph. subfract. 13	7261.9	187.4741	4.3438	372.09
Asph. subfract. 14	7700.1	198.7371	4.3502	374.01
Asph. subfract. 15	8138.6	210.0065	4.3563	375.83
Asph. subfract. 16	8577.3	221.2810	4.3620	377.55
Asph. subfract. 17	9016.2	232.5598	4.3675	379.19
Asph. subfract. 18	9455.2	243.8419	4.3727	380.75
Asph. subfract. 19	9894.3	255.1269	4.3777	382.24
Asph. subfract. 20	10333.5	266.4144	4.3825	383.67
Asph. subfract. 21	10772.7	277.7039	4.3870	385.03
Asph. subfract. 22	11212.1	288.9952	4.3914	386.34
Asph. subfract. 23	11651.5	300.2880	4.3956	387.60
Asph. subfract. 24	12091.0	311.5821	4.3997	388.82
Asph. subfract. 25	12530.5	322.8774	4.4036	389.99
Asph. subfract. 26	12970.0	334.1737	4.4074	391.12
Asph. subfract. 27	13409.6	345.4709	4.4111	392.22
Asph. subfract. 28	13849.2	356.7689	4.4146	393.27
Asph. subfract. 29	14288.8	368.0676	4.4180	394.30
Asph. subfract. 30	14728.5	379.3670	4.4214	395.29

[a] Calculated from Panuganti et al.'s correlations [27, 36]. [b] Calculated from correlations (41)−(43).

Table 2. SARA analysis (wt %) of heavy oils and bitumens, [a] asphaltene average associated molar mass [a] (M__), and average aggregation number (r_).

	Saturates	Aromatics	Resins	Asphaltenes	Solids	$\overline{M}$ g/mol
	16.3	39.8	28.5	14.6	0.8	4200
	19.4	38.1	26.7	15.3	0.5	4050
	23.1	41.7	19.5	15.1	0.6	4000
	15.4	44.4	25.0	15.0	0.2	4290
	20.5	38.0	19.6	21.8	0.1	4290
	25.0	31.1	37.1	6.8	0.0	4800
	23.2	33.9	38.2	4.7	0.0	3960

Bitumen or Heavy Oil						r
Athabasca	2.33	Cold Lake	2.25	Lloydminster	2.22	Venezuela 1	2.38	
Venezuela 2								2.38
Russia								2.67
Indonesia								2.20

[a] Ref. [16].

Table 3. Constants for determining the binary interaction parameters between asphaltene subfractions of heavy oils and bitumens and each *n*-alkane according to correlation $k_{ij} = a \cdot w_{n-\mathrm{alk}} + b$.

Heavy Oil			*n*-Pentane		*n*-Hexane			
	K	MPa	*a*	*b*	*a*	*b*	*a*	
Athabasca	296.2	0.1	0.0097	−0.0134	0.0021	−0.0078	0.0034	
Cold Lake	296.2	0.1	0.0031	−0.0064	0.0030	−0.0086	0.0022	
Lloydminster	296.2	0.1	0.0114	−0.0124	0.0019	−0.0069	0.0033	
Venezuela 1	296.2	0.1	0.0095	−0.0142			0.0052	
Venezuela 2	296.2	0.1	0.0074	−0.0113			0.0028	
Russia	296.2	0.1	0.0105	−0.0161			0.0034	
Indonesia	296.2	0.1	0.0207	−0.0254				
Athabasca	273.2	0.1					0.0103	
Athabasca	296.2	2.1					0.0068	
Athabasca	323.2	2.1					−0.0031	
Athabasca	373.2	2.1					−0.0183	0.0141
Cold Lake	296.2	2.1					0.0052	
Cold Lake	323.2	2.1					−0.0015	
Cold Lake	373.2	6.9					−0.0138	0.0128
Venezuela 1	273.2	0.1					0.0060	
Venezuela 1	296.2	0.1					0.0089	
Athabasca	296.2	0.1					0.0034	
Athabasca	296.2	2.1					0.0066	
Athabasca	296.2	6.9					0.0056	
Cold Lake	296.2	0.1					0.0021	
Cold Lake	296.2	2.1					0.0050	
Cold Lake	296.2	6.9					0.0071	

Bitumen or Heavy Oil	*T*	*P*	*n*-Heptane	*b*
Athabasca				−0.0076
Cold Lake				−0.0066
Lloydminster				−0.0065
Venezuela 1				−0.0091
Venezuela 2				−0.0070
Russia				−0.0093
Indonesia				

Athabasca	−0.0152
Athabasca	−0.0105
Athabasca	−0.0001
Athabasca	0.0141
Cold Lake	−0.0086
Cold Lake	−0.0008
Cold Lake	0.0128
Venezuela 1	−0.0155
Venezuela 1	−0.0139
Athabasca	−0.0077
Athabasca	−0.0102
Athabasca	−0.0093
Cold Lake	−0.0064
Cold Lake	−0.0083
Cold Lake	−0.0096

FIGURE CAPTIONS

Fig. 1. Flow diagram to calculate liquid-liquid equilibrium for asphaltene precipitation (adapted from Sabbagh [31]).

Fig. 2. Flow diagram for Rachford-Rice flash calculation (adapted from Sabbagh [31]).

Fig. 3. PC-SAFT parameters m , σ, and ε/k as a function of molar mass for saturates pseudocomponent and asphaltene subfractions.

Fig. 4 PC-SAFT parameters m , σ, and ε/k as a function of molar mass for saturates, aromatics, and resins pseudo-components, and asphaltene subfractions.

Fig. 5. Binary interaction parameters as a function of *n*-alkane mass fraction from Athabasca bitumen diluted with *n*-alkanes at 296.2 K and 0.1 MPa.

Fig. 6. Binary interaction parameters as a function of *n*-alkane mass fraction from Athabasca bitumen diluted with *n*-heptane at 273.2 K and 0.1 MPa, and at 296.2, 323.2 and 373.2 K all at 2,1 MPa.

Fig. 7. Experimental and calculated fractional yield from Athabasca bitumen diluted with *n*-alkanes at 296.2 K and 0.1 MPa. Symbols are experimental data from Sabbagh et al. [16], solid lines are calculated fractional yields with the PC-SAFT EoS, and dotted line is the solids content.

Fig. 8. Experimental and calculated fractional yield from Cold Lake bitumen diluted with *n*-alkanes at 296.2 K and 0.1 MPa. Symbols are experimental data from Sabbagh et al. [16], solid lines are calculated fractional yields with the PC-SAFT EoS, and dotted line is the solids content.

Fig. 9. Experimental and calculated fractional yield from Lloydminster heavy oil diluted with *n*-alkanes at 296.2 K and 0.1 MPa. Symbols are experimental data from Sabbagh et al. [16], solid lines are calculated fractional yields with the PC-SAFT EoS, and dotted line is the solids content.

Fig. 10. Experimental and calculated fractional yield from Venezuela 1 heavy oil diluted with *n*-alkanes at 296.2 K and 0.1 MPa. Symbols are experimental data from Sabbagh et al. [16], solid lines are calculated fractional yields with the PC-SAFT EoS, and dotted line is the solids content.

Fig. 11. Experimental and calculated fractional yield from Venezuela 2 heavy oil diluted with *n*-alkanes at 296.2 K and 0.1 MPa. Symbols are experimental data from Sabbagh et al. [16], solid lines are calculated fractional yields with the PC-SAFT EoS, and dotted line is the solids content.

Fig. 12. Experimental and calculated fractional yield from Russia bitumen diluted with *n*-alkanes at 296.2 K and 0.1 MPa. Symbols are experimental data from Sabbagh et al. [16], solid lines are calculated fractional yields with the PC-SAFT EoS, and dotted line is the solids content.

Fig. 13. Experimental and calculated fractional yield from Indonesia bitumen diluted with *n*-pentane at 296.2 K and 0.1 MPa. Symbols are experimental data from Sabbagh et al. [16], solid lines are calculated fractional yields with the PC-SAFT EoS, and dotted line is the solids content.

Fig. 14. Experimental and calculated fractional yield from Athabasca bitumen diluted with *n*-heptane at 296.2 K and 0.1 MPa and at 296.2, 323.2, and 373.2 K all at 2.1 MPa. Symbols are experimental data from Sabbagh et al. [16], solid lines are calculated fractional yields with the PC-SAFT EoS, and dotted line is the solids content.

Fig. 15. Experimental and calculated fractional yield from Cold Lake bitumen diluted with *n*-heptane at 296.2 K and 2.1 MPa, 323.2 K and 2.1 MPa, and 373.2 K and 6.9 MPa. Symbols are experimental data from Sabbagh et al. [16], solid lines are calculated fractional yields with the PC-SAFT EoS, and dotted line is the solids content.

Fig. 16. Experimental and calculated fractional yield from Venezuela 1 bitumen diluted with *n*-pentane at 273.2 and 296.2 K both at 0.1 MPa. Symbols are experimental data from Sabbagh et al. [16], solid lines are calculated fractional yields with the PC-SAFT EoS, and dotted line is the solids content.

Fig. 17. Experimental and calculated fractional yield from Athabasca bitumen diluted with *n*-heptane at 296.2 K and 0.1, 2.1, and 6.9 MPa. Symbols are experimental data from Sabbagh et al. [16], solid lines are calculated fractional yields with the PC-SAFT EoS, and dotted line is the solids content.

Fig. 18. Experimental and calculated fractional yield from Cold Lake bitumen diluted with *n*-heptane at 296.2 K and 0.1, 2.1, and 6.9 MPa. Symbols are experimental data from Sabbagh et al. [16], solid lines are calculated fractional yields with the PC-SAFT EoS, and dotted line is the solids content.

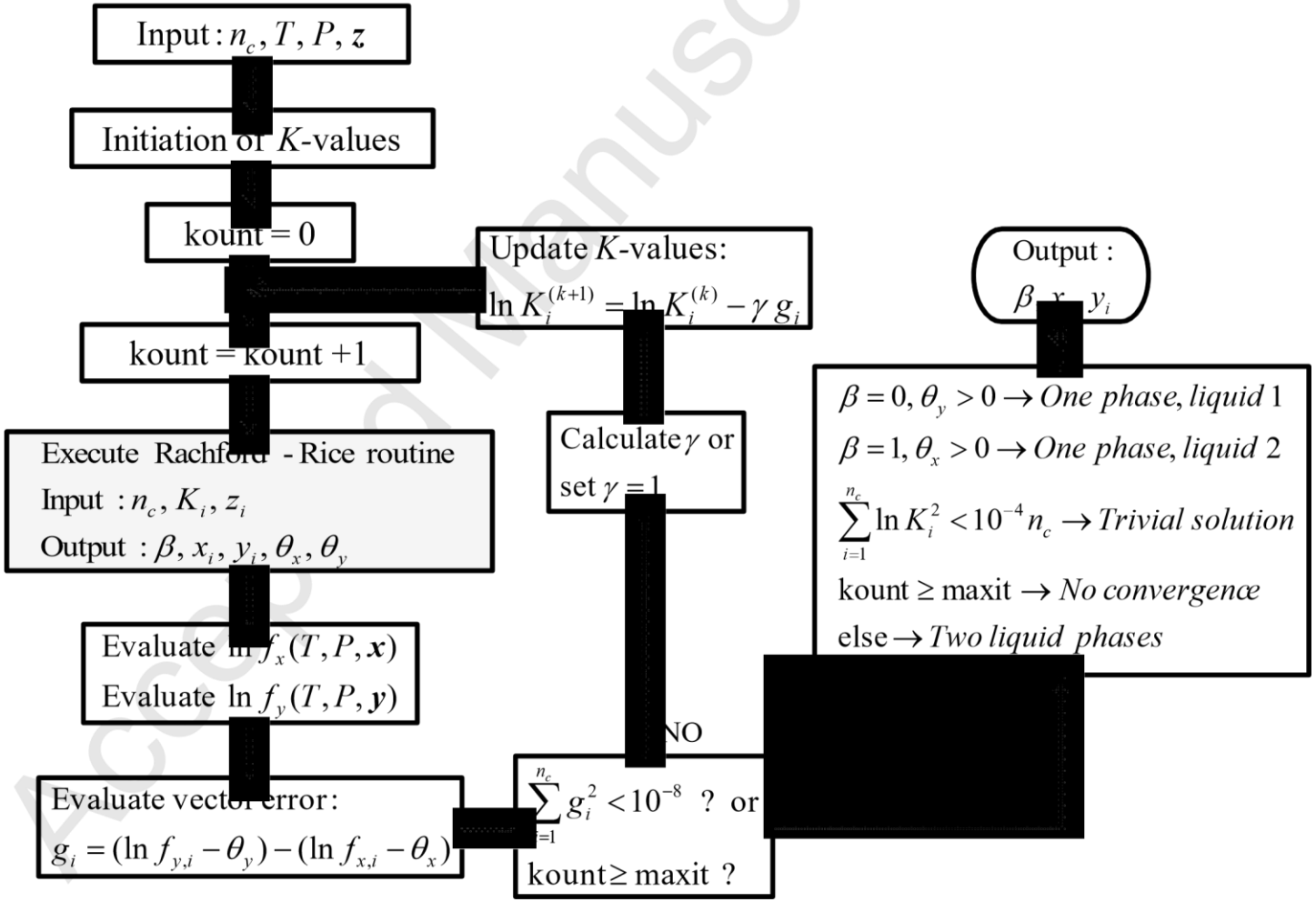

Figure 1. (*Zúñiga-Hinojosa et al.*)

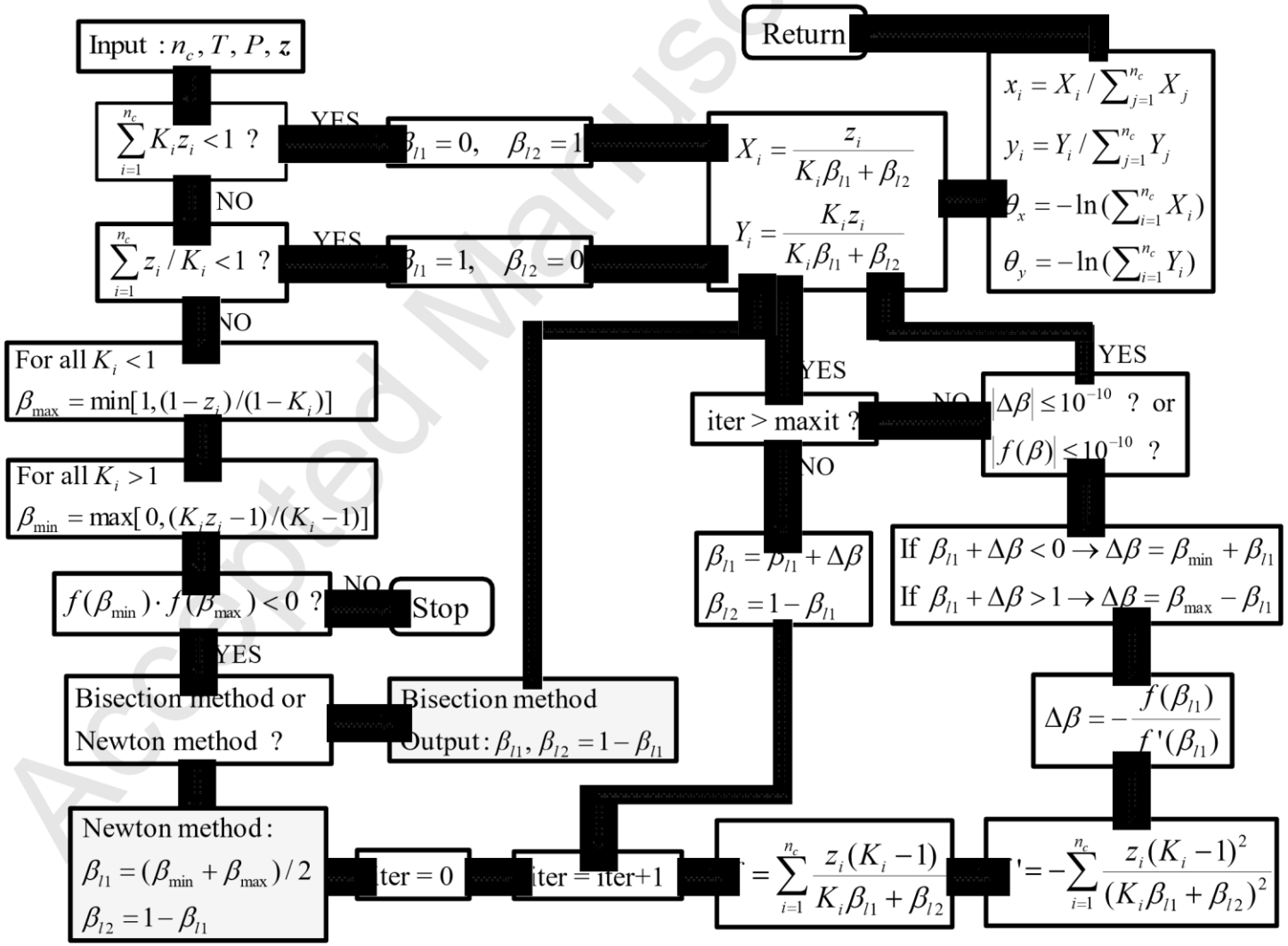

Figure 2. (*Zúñiga-Hinojosa et al.*)

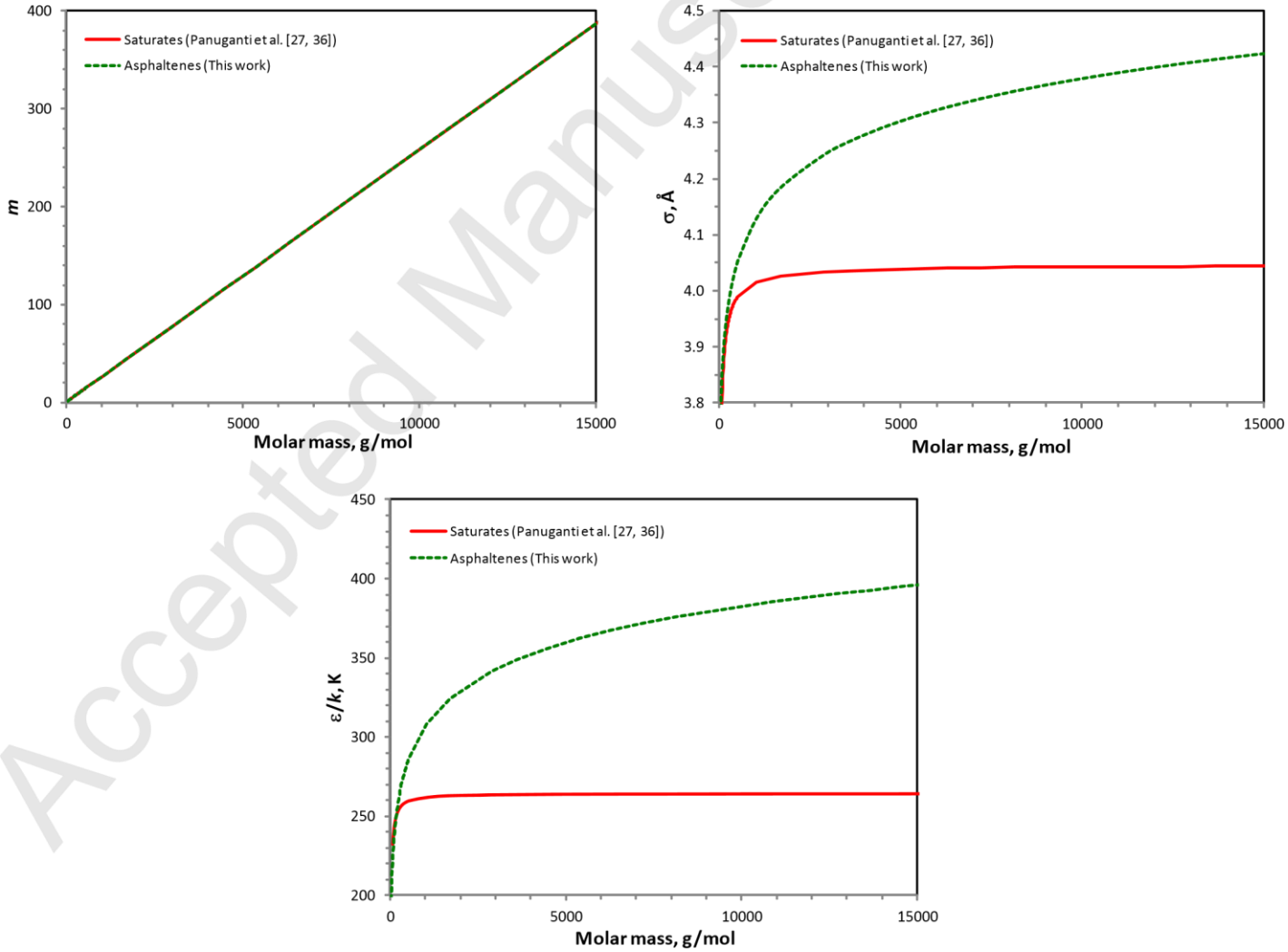

Figure 3. (*Zúñiga-Hinojosa et al.*)

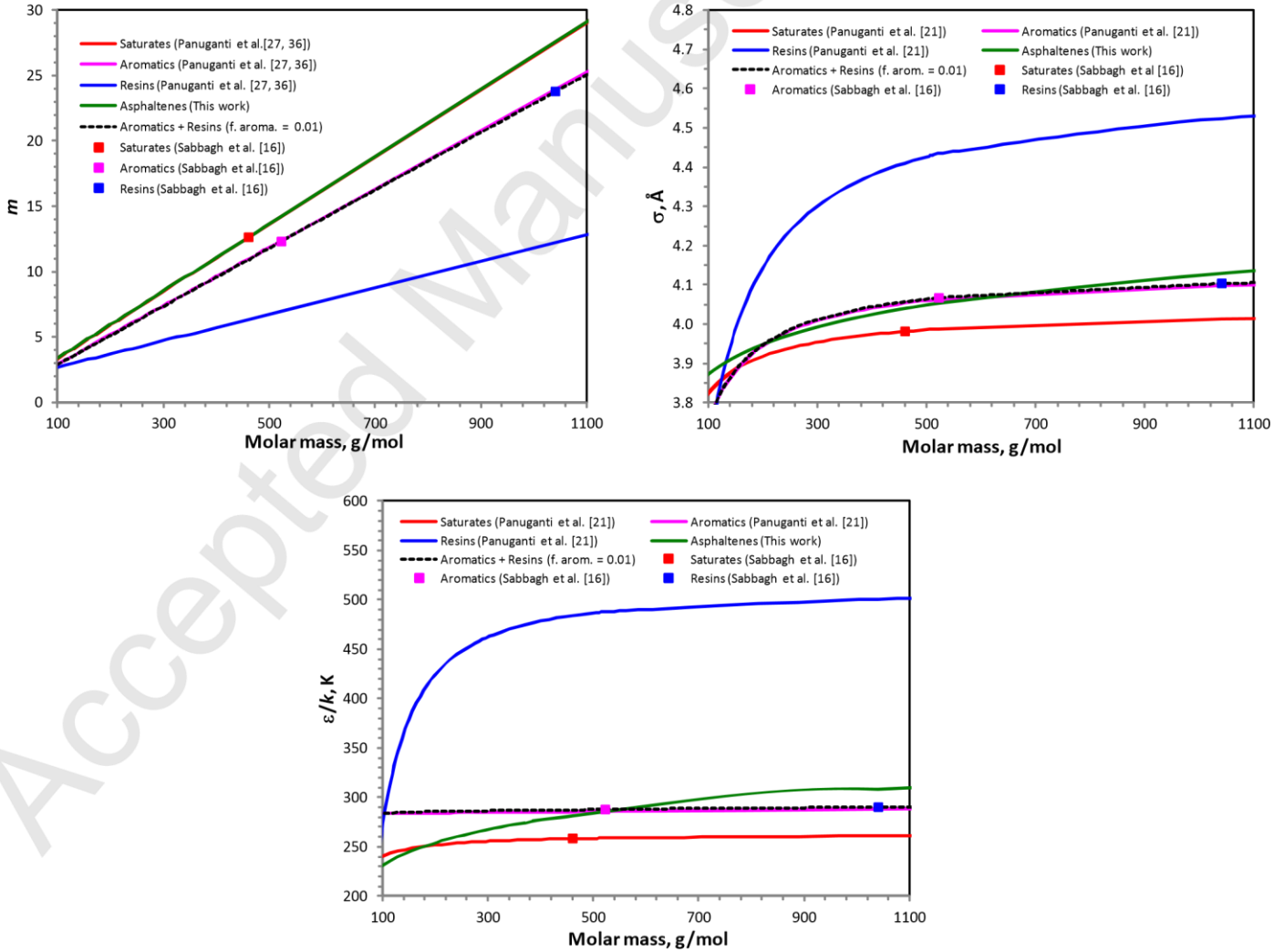

Figure 4. (*Zúñiga-Hinojosa et al.*)

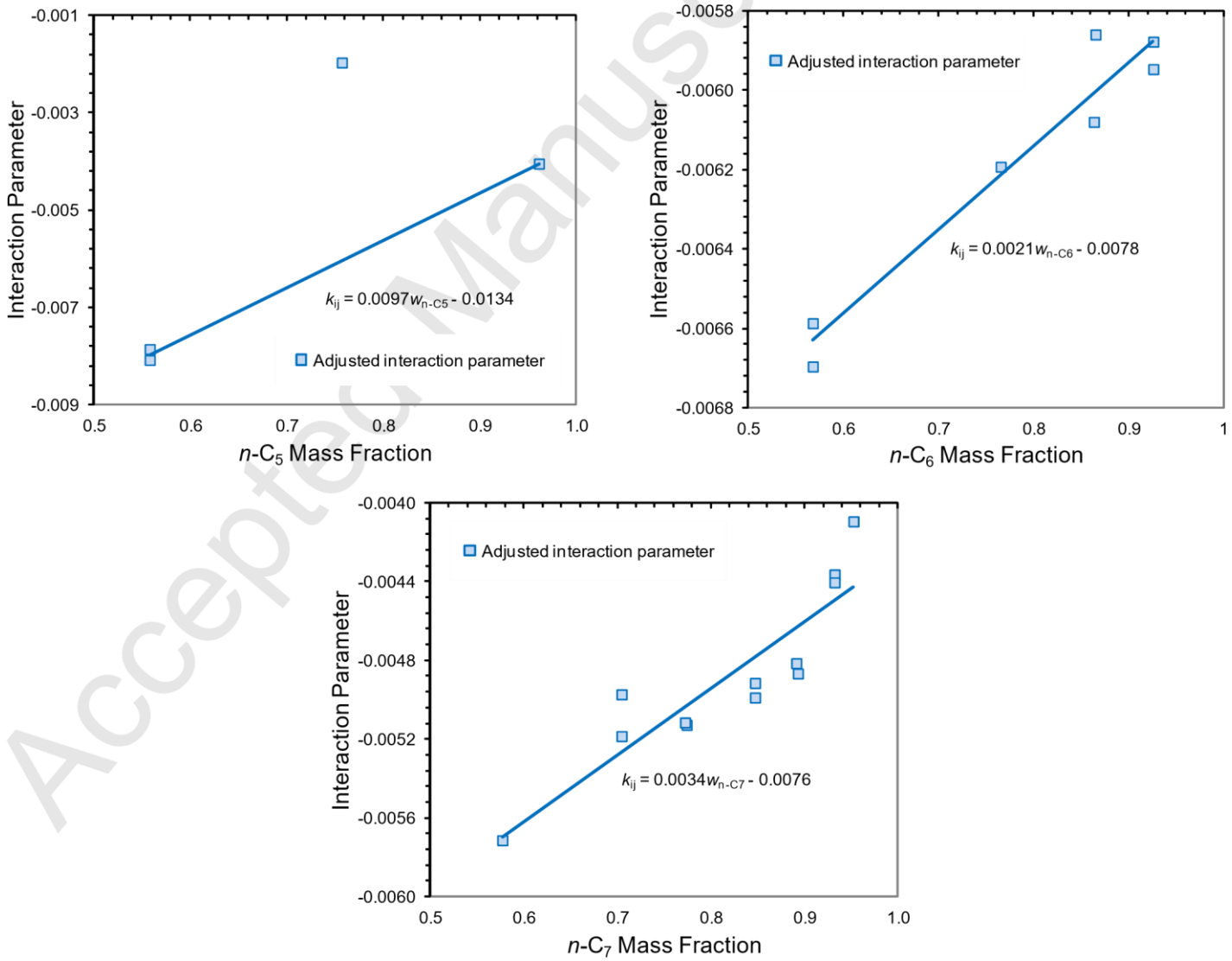

Figure 5. (*Zúñiga-Hinojosa et al.*)

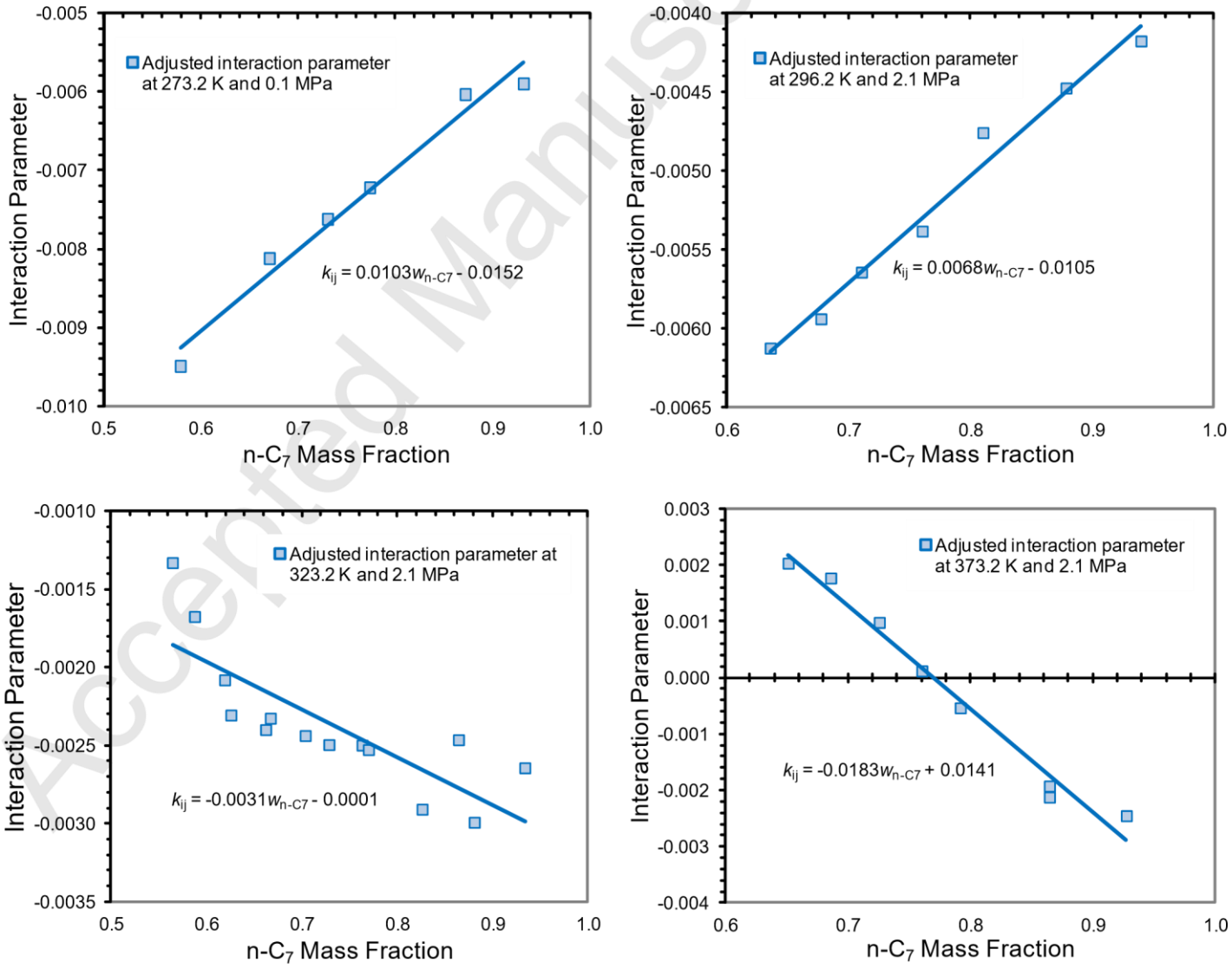

Figure 6. (*Zúñiga-Hinojosa et al.*)

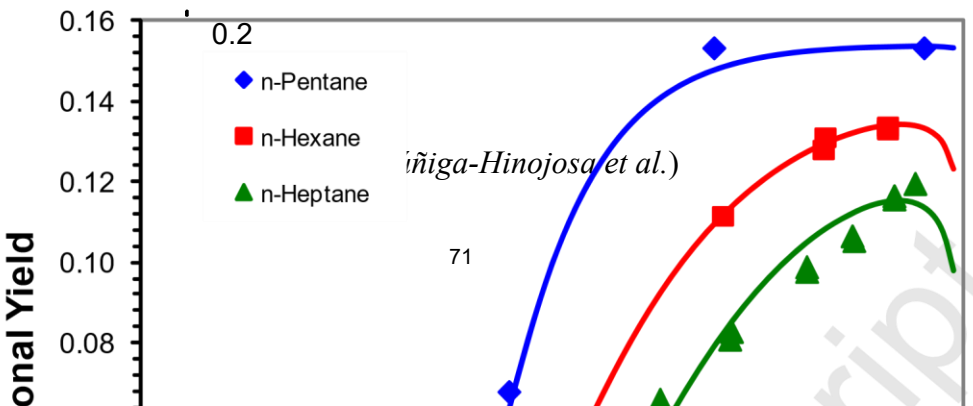

Figure 8. (

0.2

Zúñiga-Hinojosa et al.)

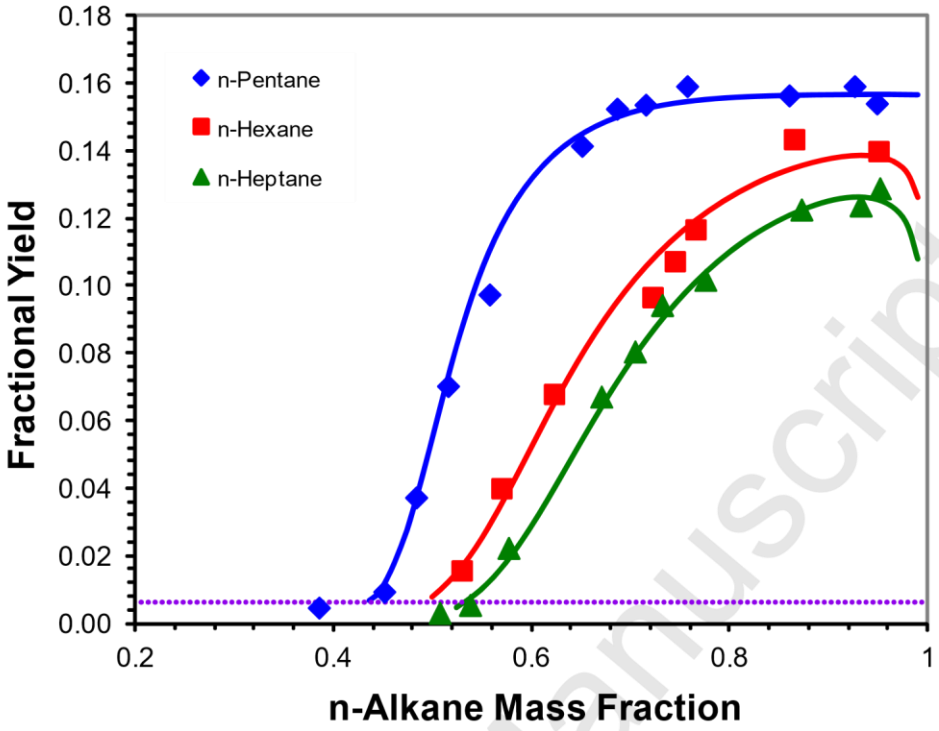

Figure 9. (*Zúñiga-Hinojosa et al.*)

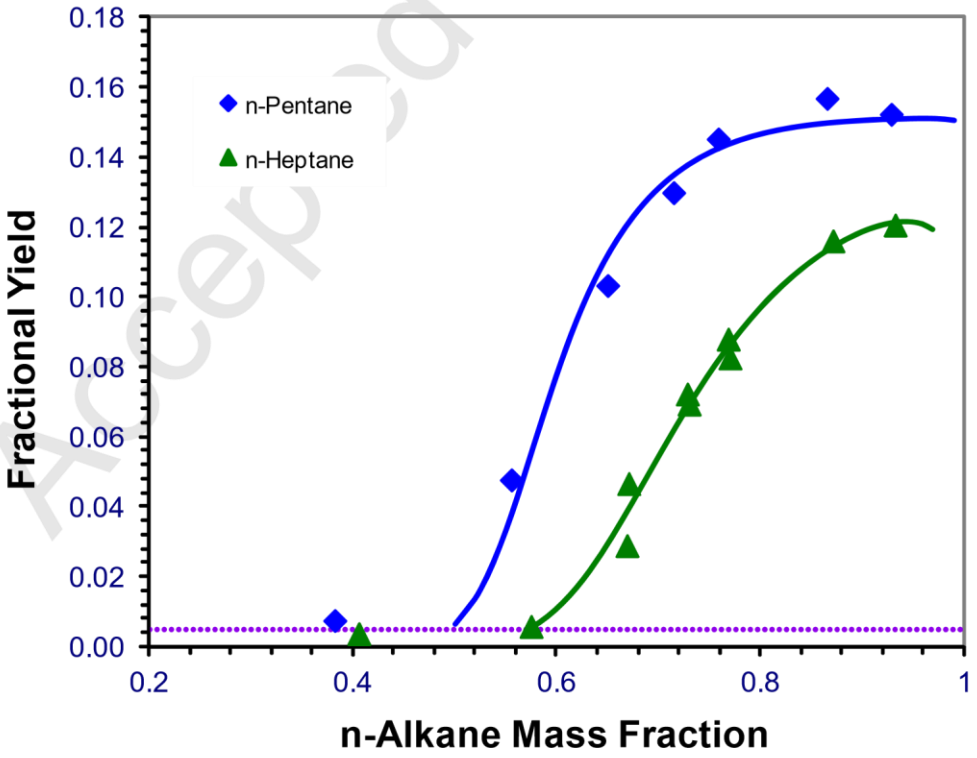

Figure 10. (*Zúñiga-Hinojosa et al.*)

0.2

Zúñiga-Hinojosa et al.)

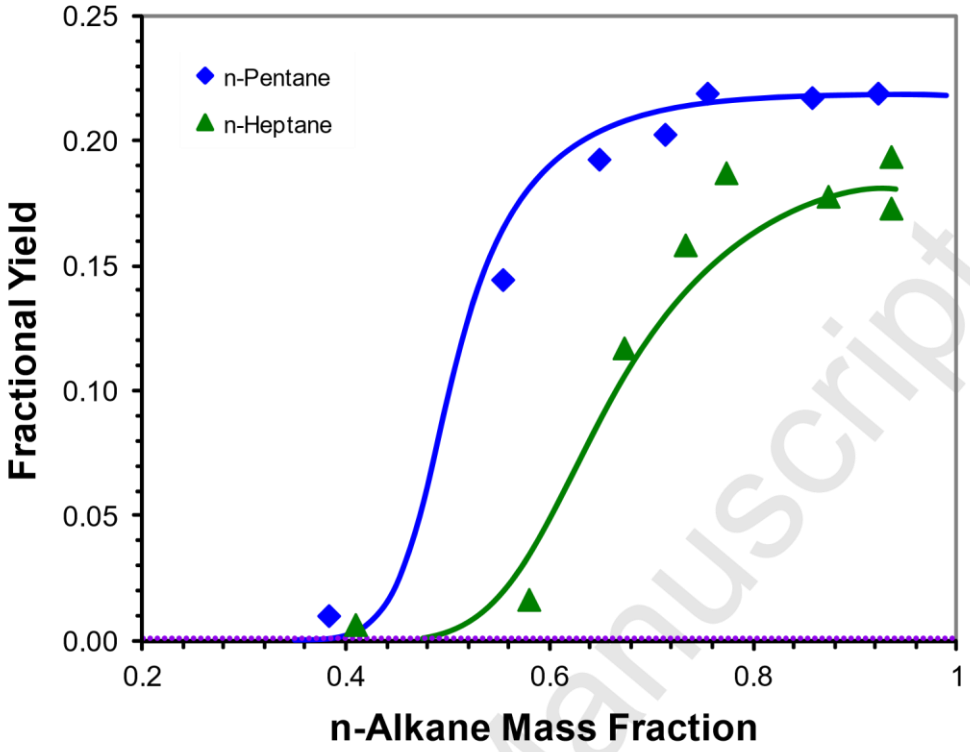

Figure 11. (*Zúñiga-Hinojosa et al.*)

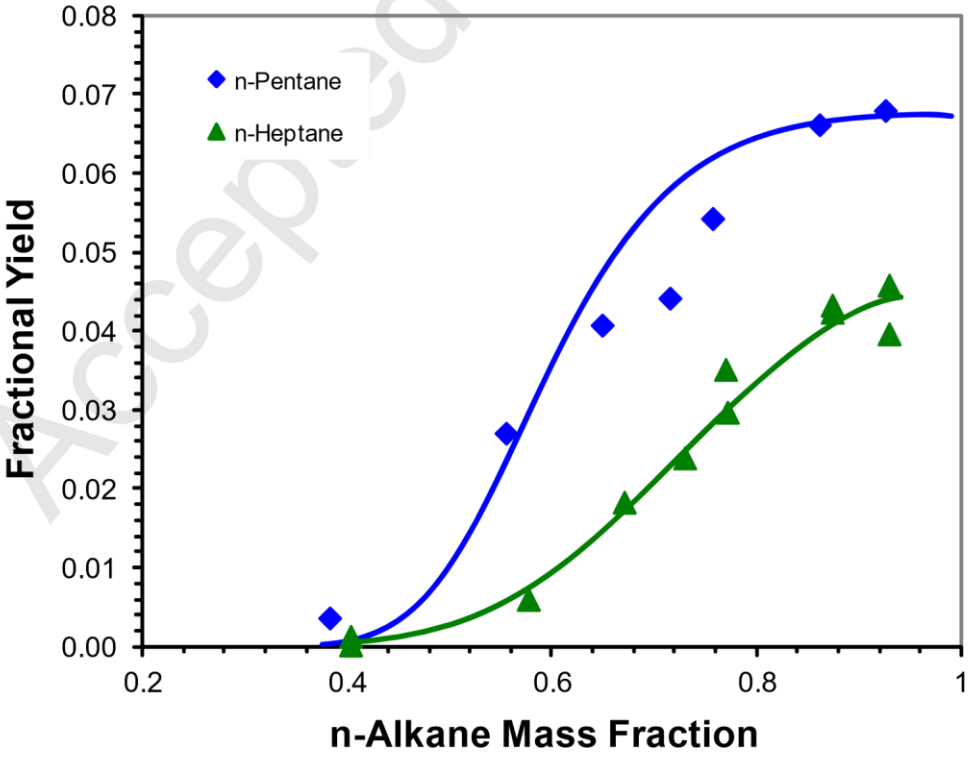

Figure 12. (

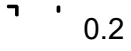

Zúñiga-Hinojosa et al.)

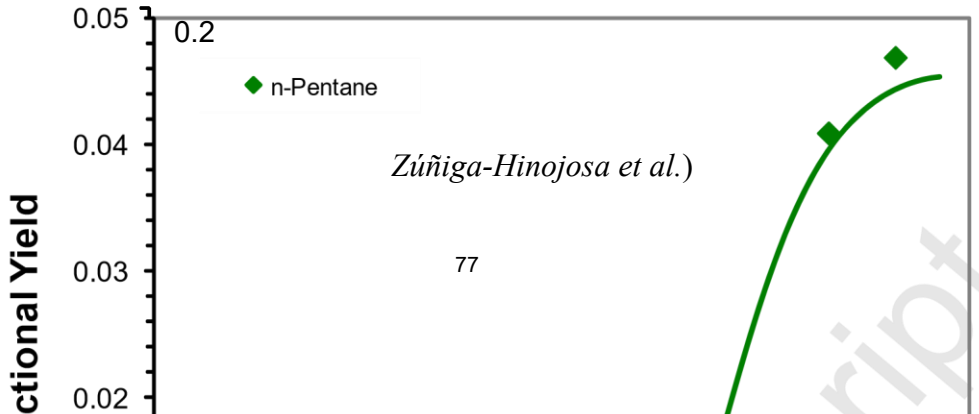

Zúñiga-Hinojosa et al.)

77

Figure 14. (

0.2

Zúñiga-Hinojosa et al.)

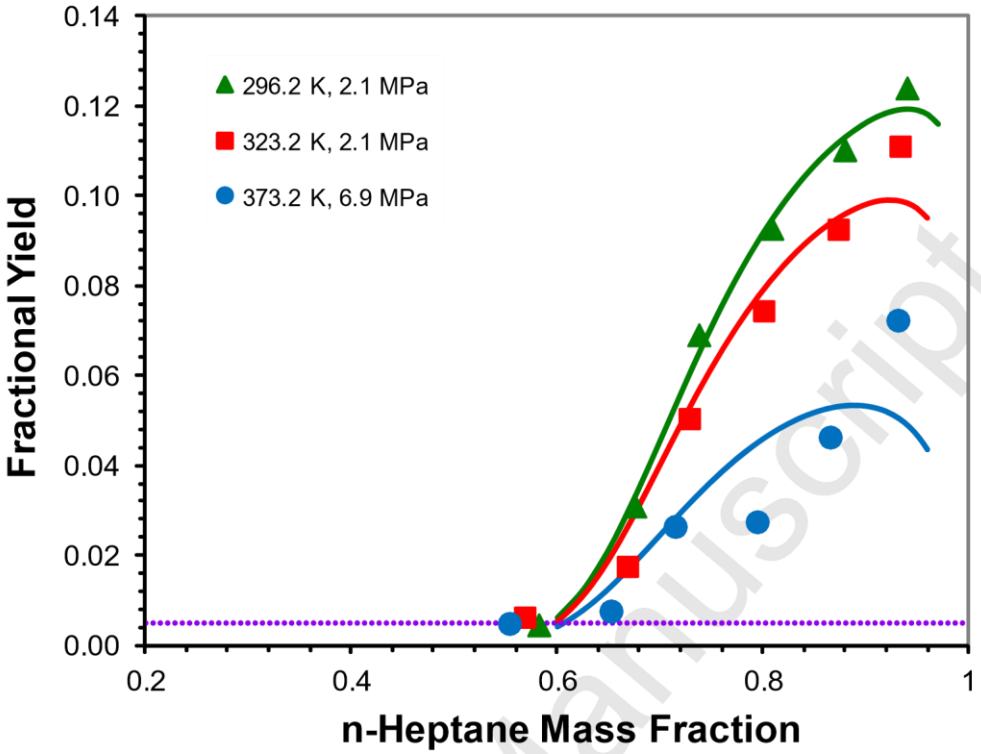

Figure 15. (*Zúñiga-Hinojosa et al.*)

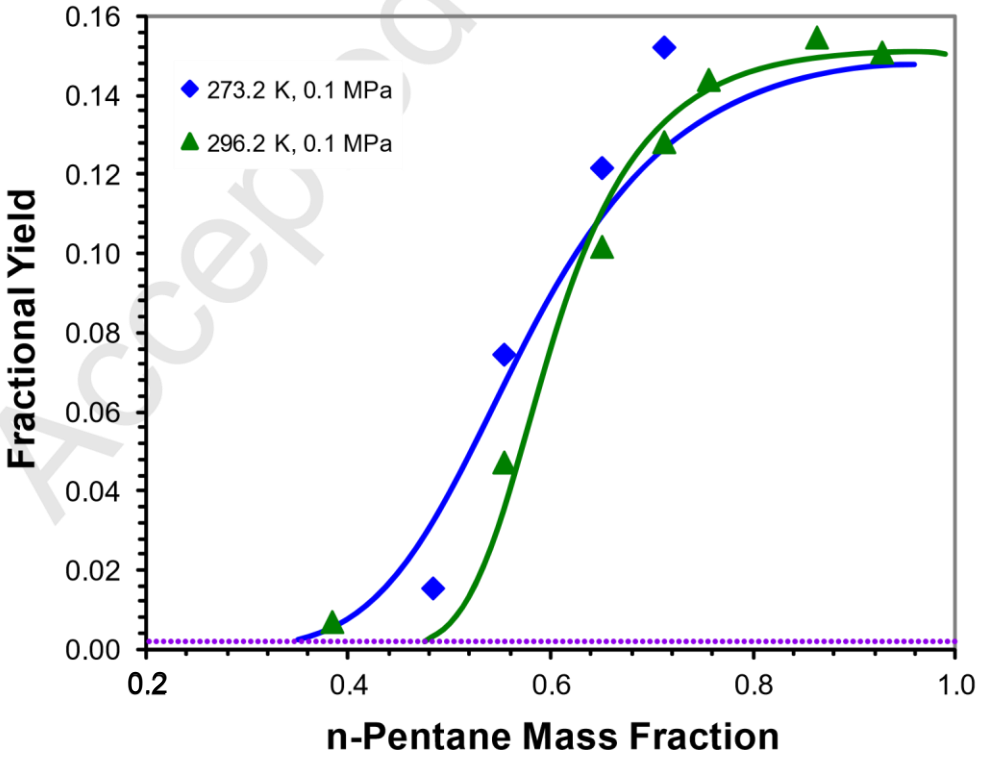

Zúñiga-Hinojosa et al.)

Figure 16. (

0.2

Zúñiga-Hinojosa et al.)

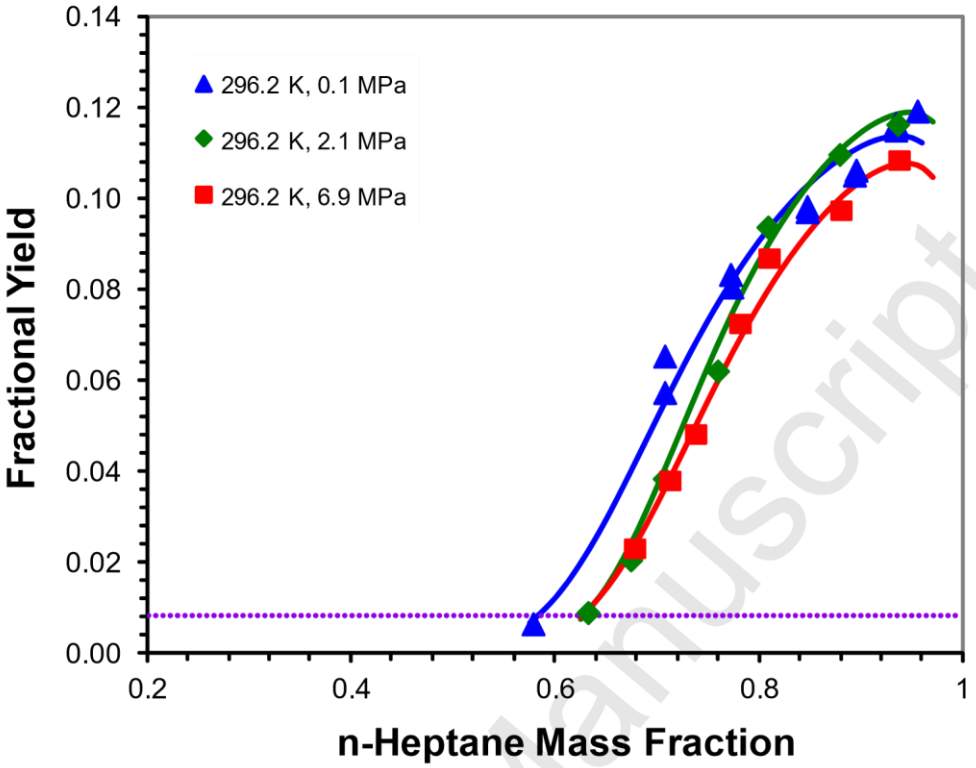

Figure 17. (*Zúñiga-Hinojosa et al.*)

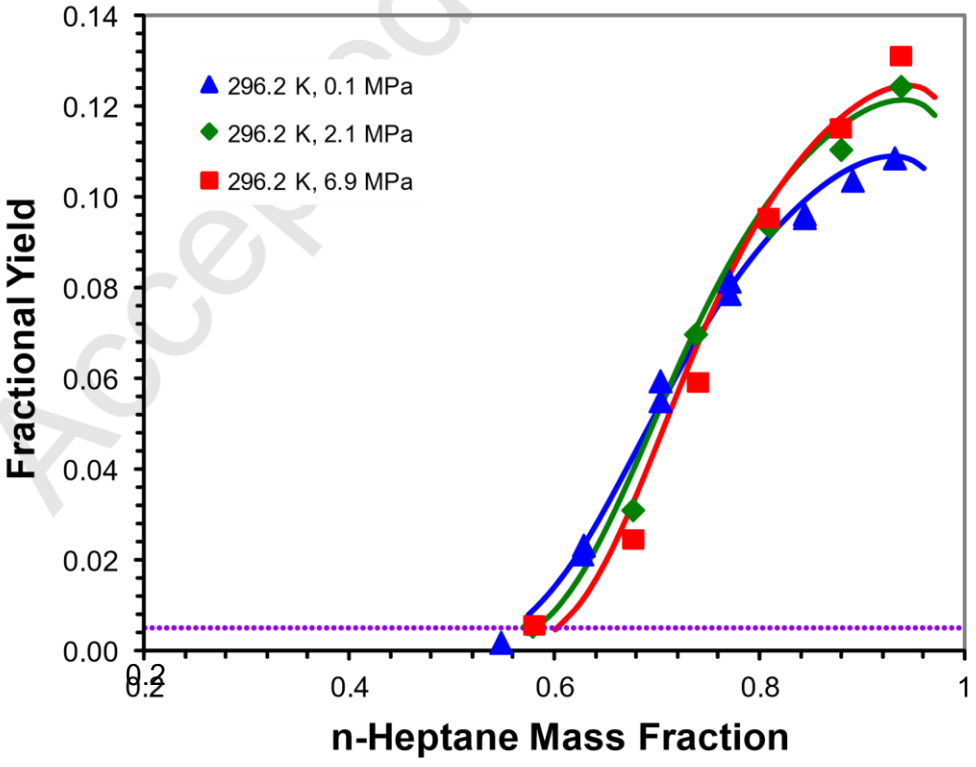

Zúñiga-Hinojosa et al.)

Figure 18. (

0.2

Zúñiga-Hinojosa et al.)